Sgr A* and its environment: confronting simulations with observations

Q. Daniel Wang

(University of Massachusetts)

in collaboration with

Shawn Roberts (Umass), Yan-Fei Jiang (CfA), Jerry Ostriker (Columbia/Princeton), Christopher Russell (GSFC/NASA), Cuadra, Jorge (Pontificia Universidad Católica de Chile), etc.

The Galactic center in near-IR

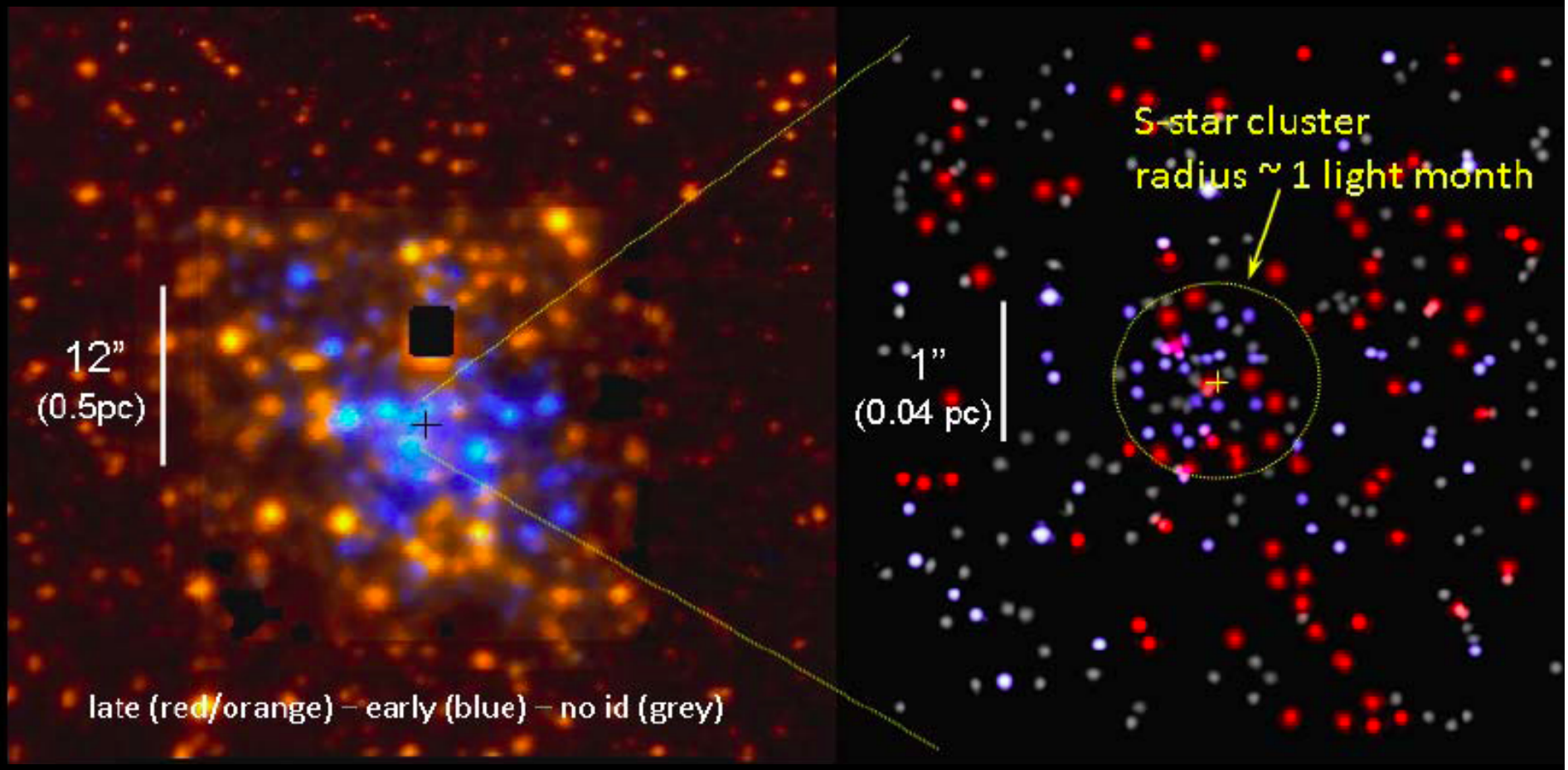

From Genzel et al. (2010)

Sgr A* and its vicinity: 1-9 keV image

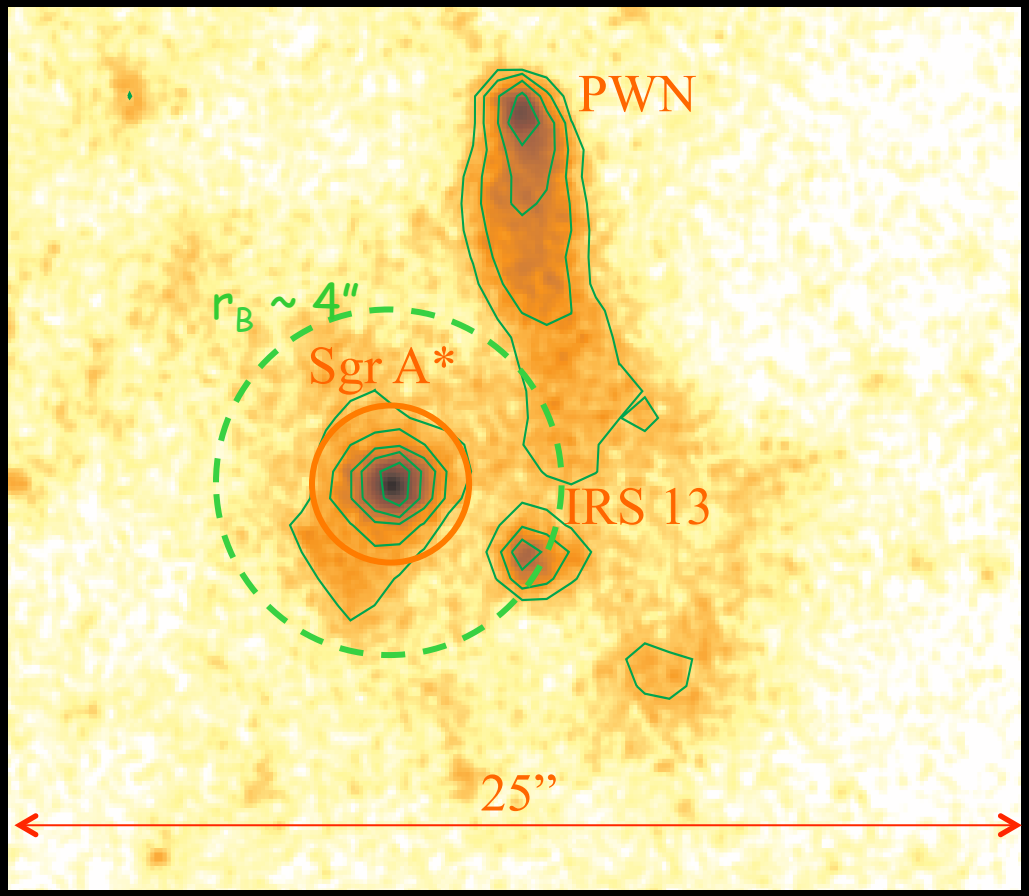

- $M_{BH}=4\times10^6 M_\odot$
- $L_x= 3\times10^{33}$ erg/s,
  or ~ $10^{-11} L_E$
- L_{bol}= a few $\times10^{36}$ erg/s, mostly in radio to submm.
- What is the mode of the accretion?
- What determines the luminosity?
- What is the possible outflow?

If we have answers to these questions, we may understand a large class of ultra-dim galactic nuclei.

Wang et al. (2013, Science)

Temporal decomposition of the Sgr A* X-ray data (2012 XVP)

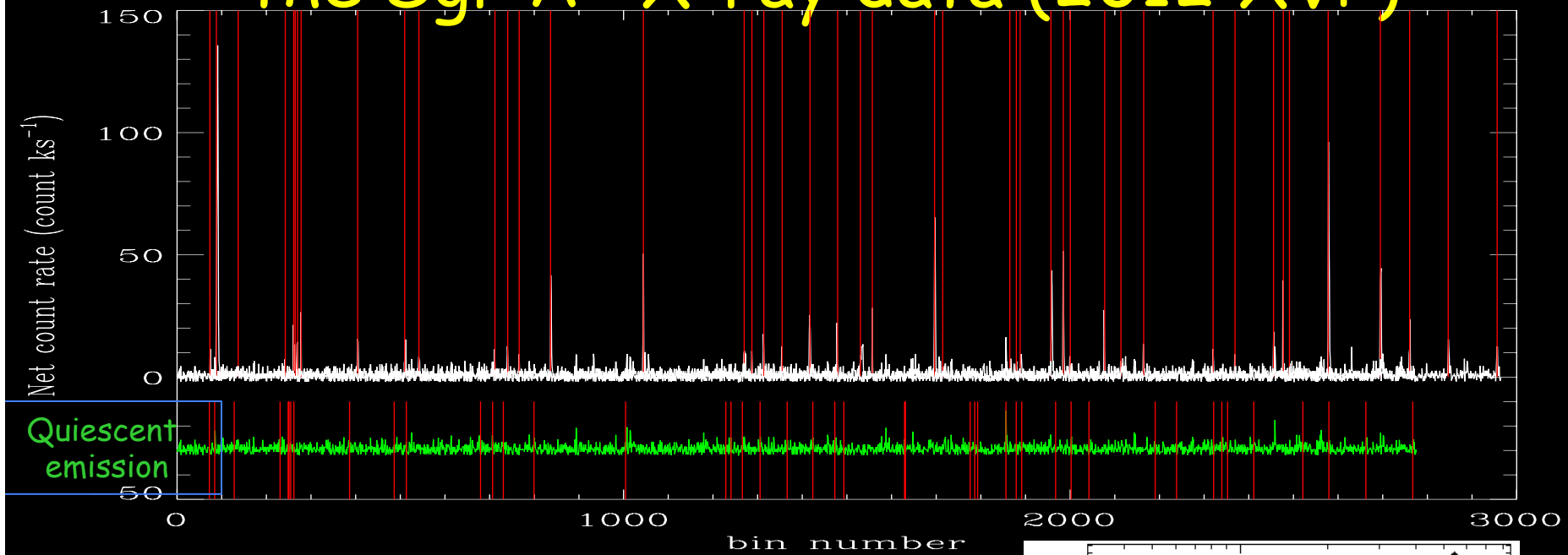

- Detected flares have a fluence distribution dN/dF ~ $F^{-1.5}$ and account for ~1/3 of the total X-ray flux of Sgr A* (Neilsen et al. 13; Yuan & Wang 16).
- The log-normal dispersion of the intrinsic duration σ_{ET}~0.25.

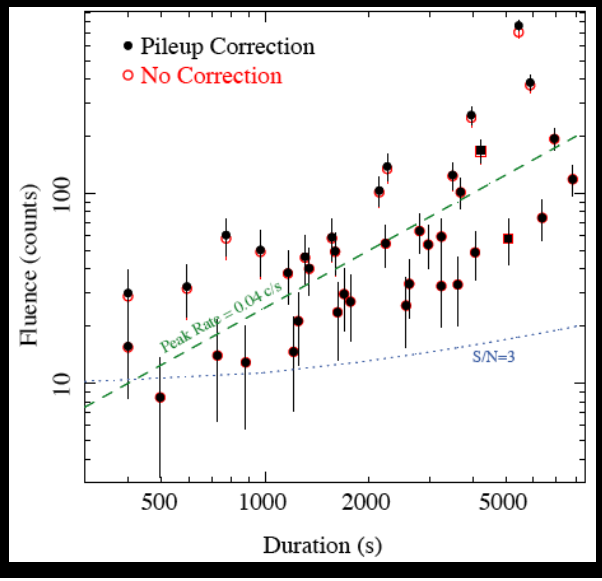

Flare and quiescent emissions: spatial and spectral properties

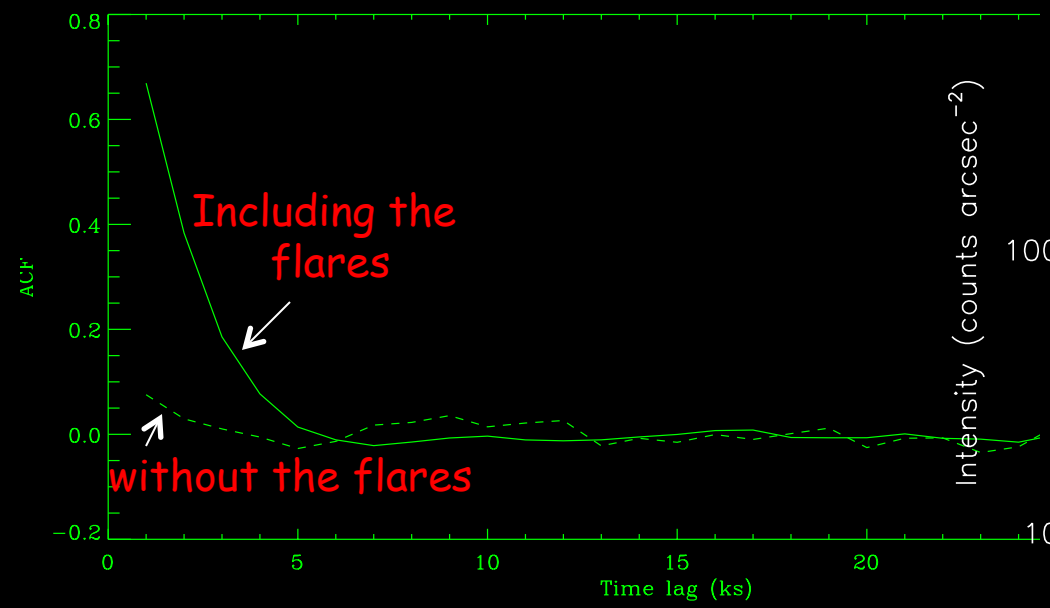

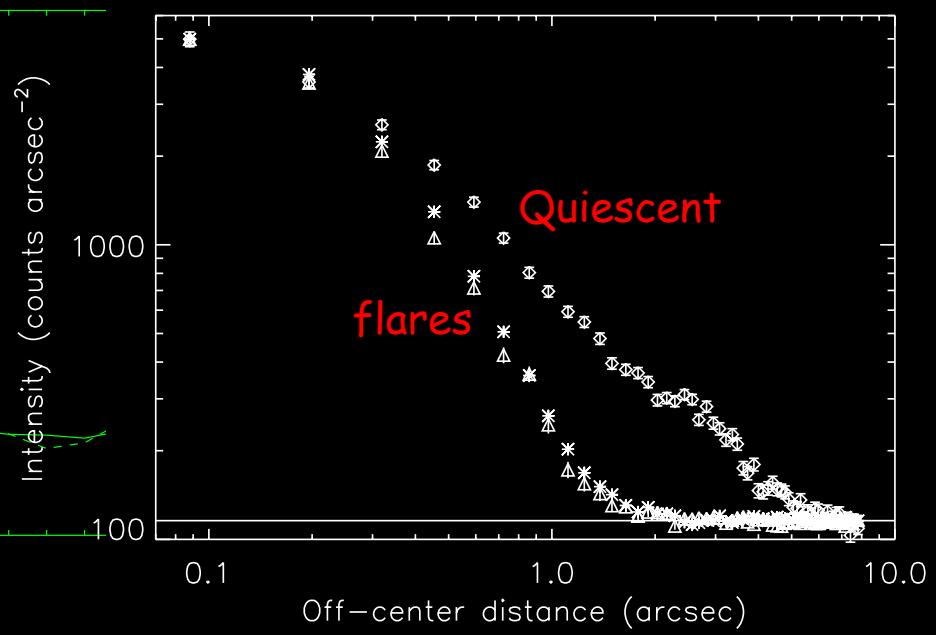

- The flare emission is point-like.
- The flare spectra show no sign for any lines.
- The quiescent emission is extended on 1″-5″ scales.

Wang et al. (2013, Science)

Spatial decomposition of the Sgr A* quiescent X-ray emission

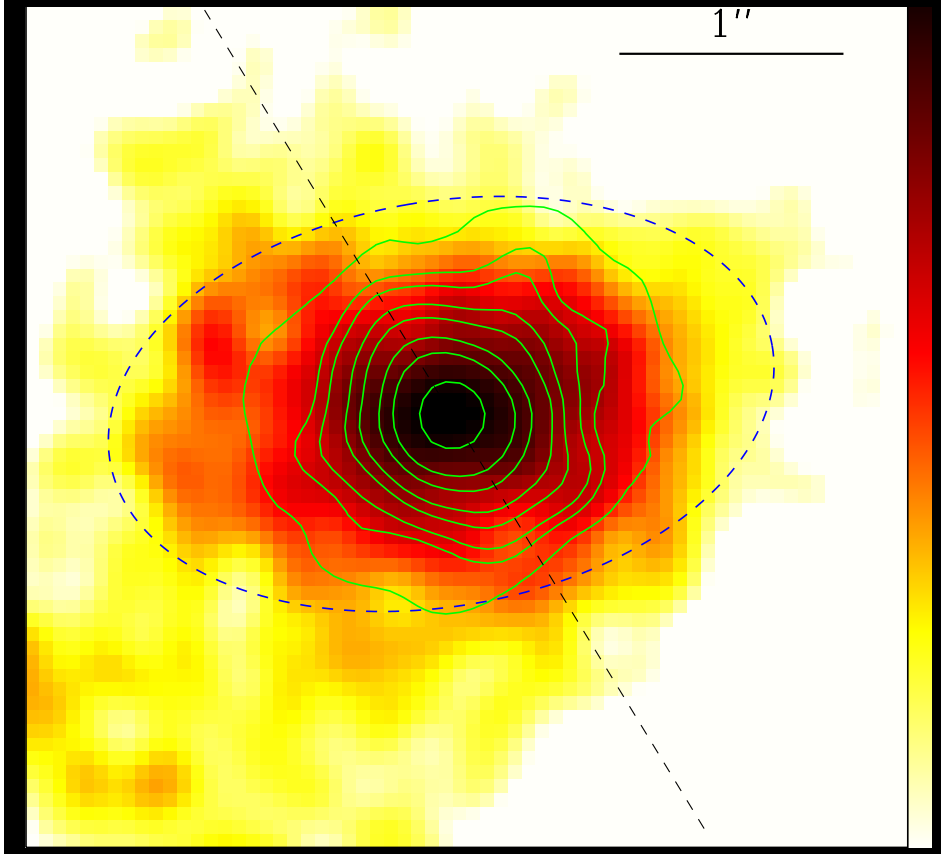

- Point-like component accounting for < 20% of the total flux within 1.5″ radius.
- Extended component with an elongated morphology on 1″ scales.
- Elongation direction consistent with the orientation of the clockwise massive stellar disk.

Wang et al. (2013, Science)

Key Remaining Questions

- Are the X-ray data consistent with the shocked stellar wind accretion scenario?
- What can we learn about the morphology, as well as the density and temperature distributions of the accretion flow.
- What constraints can we obtain on other X-ray-emitting components, especially on the unresolved emission near the SMBH?
- What inferences can we derive about the mass and energetics of the outflow work
- How does the outflow affect the environment?
- How has Sgr A* activity changed with time?

X-ray emission line spectroscopy

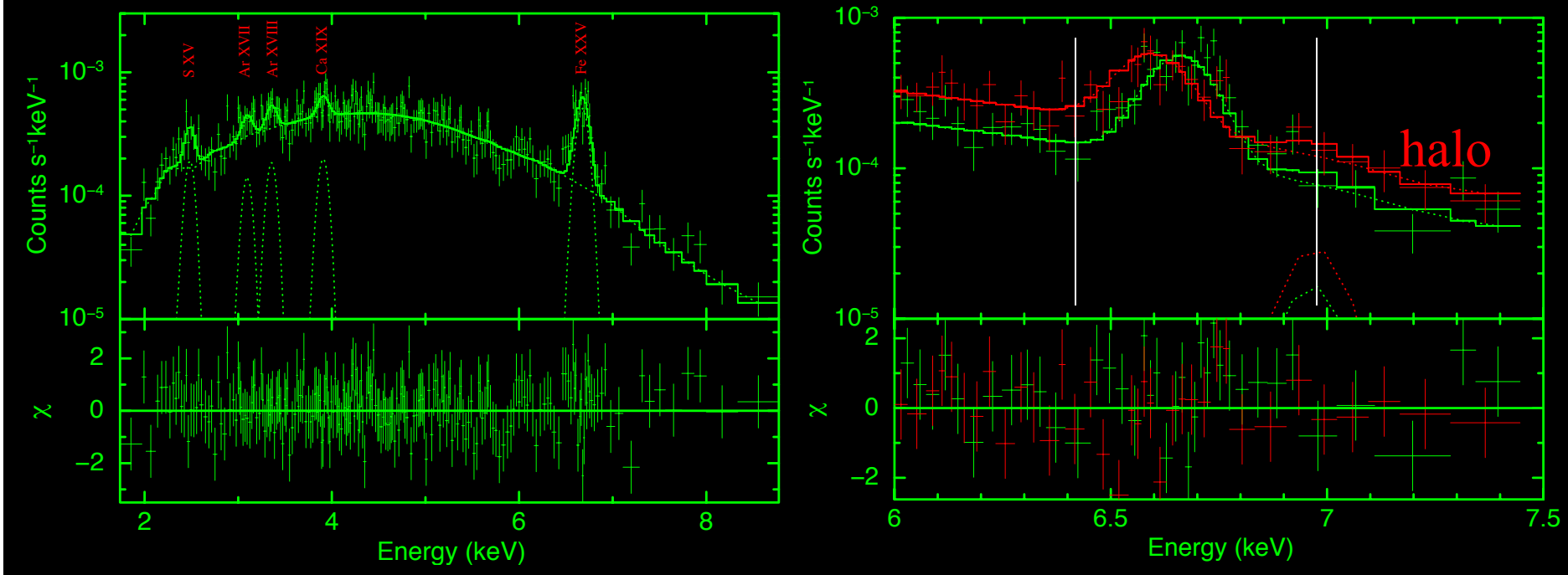

Major Classes of Radiatively Inefficient Accretion Flow (RIAF)

- Advection-dominated accretion flow (ADAF; Narayan & Yi 1994)
- Adiabatic inflow-outflow solution (ADIOS; Blandford & Begelman 1999, 2004; Begelman 2012).
- Convection-dominated accretion flow (CDAF; Quataert & Gruzinov 2000)

These self-similar solutions are partly consistent with various HD and MHD simulations (e.g., Radiating Rotating Inflow-Outflow Solutions, RRIOS; Ostriker's talk).

X-ray spectral model of RIAF solutions

$$T = T_o(r_o/r)^{\theta}$$
$$n = n_o(r_o/r)^{3/2-s}$$
$$\dot{M} = \dot{M}_o(r/r_o)^{s}$$
$$dEM/d\log(T) \propto (T_o/T)^{\gamma}$$
$$(\text{where } \gamma = 2s/\theta)$$

s varies from 0 (ADAF) to 1 (ADIOS).

This component applies for r $>10^2$ R_s.

A bremsstrahlung continuum with fixed kT_i=100 keV is added for electrons with an saturated energy.

The two component model is used to fit the observed spectrum with the key parameters: γ, abundance, and the two normalizations; weak dependence on T_o.

Spectral testing of RIAF solutions

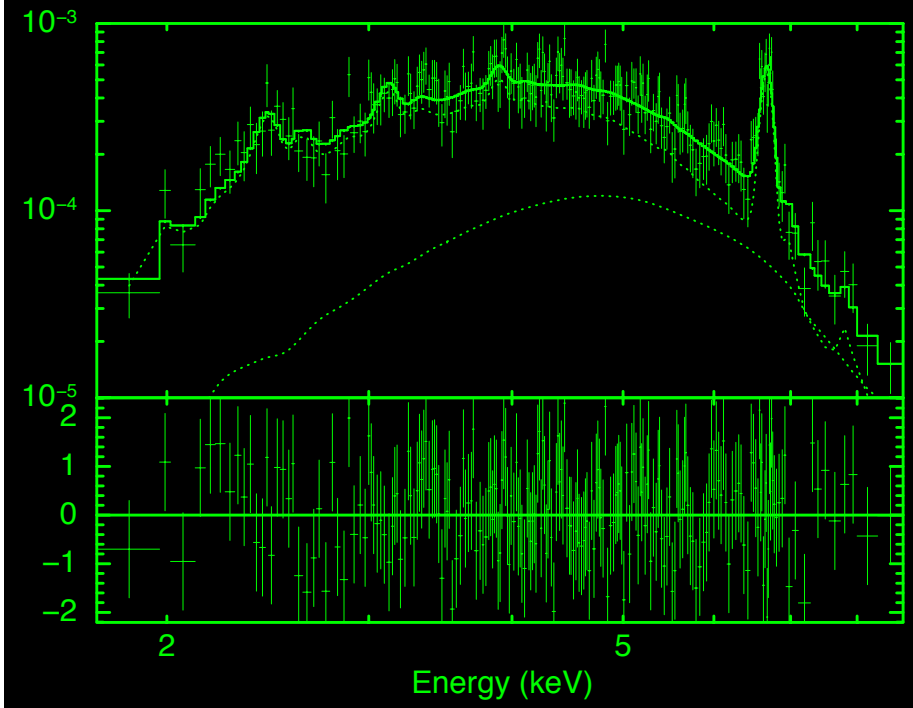

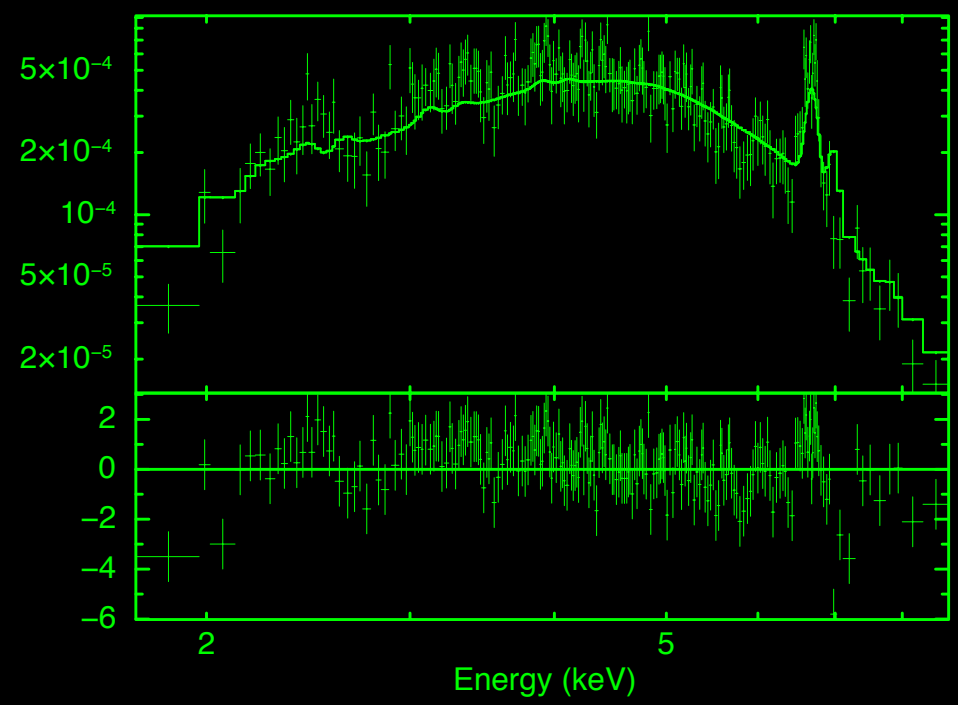

- The best-fit s=1.0(0.7-1.2) (for θ~1) is consistent with the exact prediction of ADIOS; both the fitted abundance and N_H are also as expected.
- Smaller s would give a too large FeXXVI/FeXXV Kα ratio and a too flat spectral shape to be consistent with obs.

The X-ray spectrum is consistent with the ADIOS

- $T_o \sim 10^7$K at the outer radius $r_o \sim 10^5 R_s$.
- $n = 1 \times 10^2$ cm^{-3} $(r_o/r)^{1/2}\, \xi^{-1/2}$.
- Combining the above with the mass rate limits from the Faraday rotation measure →

$\dot{M} \sim 10^{-4}\, (r_o/r)^{-1}\, M_\odot$/yr all the way down to $r \sim 10\text{-}10^2\, R_s$.

- The 100 keV bremsstrahlung component accounts for ~20% of the total flux.

Results from spectral analysis

- The bulk of the emission arises from outer regions ($r \sim 10^4$-10^5 r_s) of the accretion flow toward the SMBH.
- The point-like component accounts for at most ~20% of the total flux, in sharp contrast to AGNs, in which the innermost regions dominate.
- Detection of Ka line emission from hot S, Ar, and Ca, as well as Fe known previously, in the quiescent spectrum.
- A flat density distribution is inferred from the global spectral fit, as well as Fe XXVI/FeXXV K ratio (< 0.06) . Or > 99% of the initially captured matter is ejected in the outer region.

Wang et al. (2013, Science)

Interaction of the SMBH with the environment

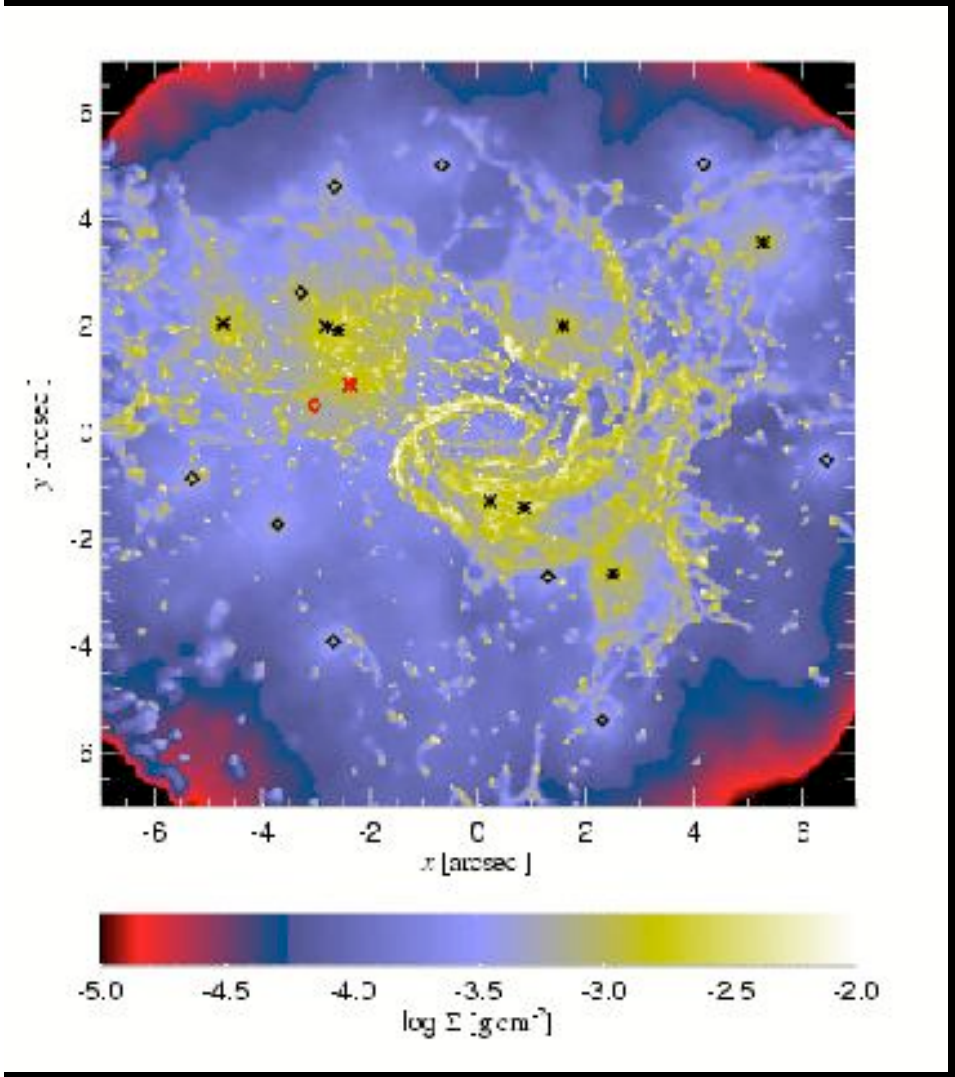

Existing simulations account for only stellar winds from massive stars (Cuadra+08):

- Hydrodynamics – SPH, down to 10^4 r_s.
- 30 Wolf-Rayet stars within 12″
- Orbits, wind properties known moderately well
- dM/dt ~ 0.5-10 x 10^{-5} Msun/yr
- Largest mass-loss-rate objects in vicinity
- v_∞ ~ 600-2500 km/s
- Shocks -> thermal X-rays

Cuadra, Nayakshin, & Wang (2016)

Column Density

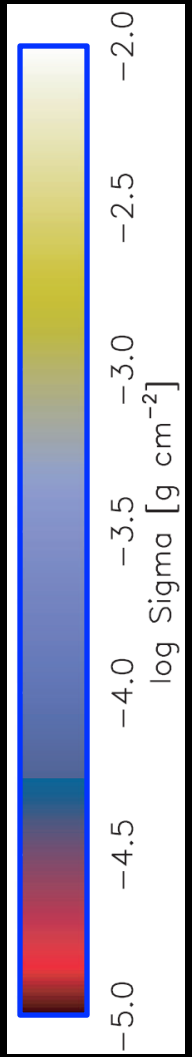

±6″

Cuadra+08

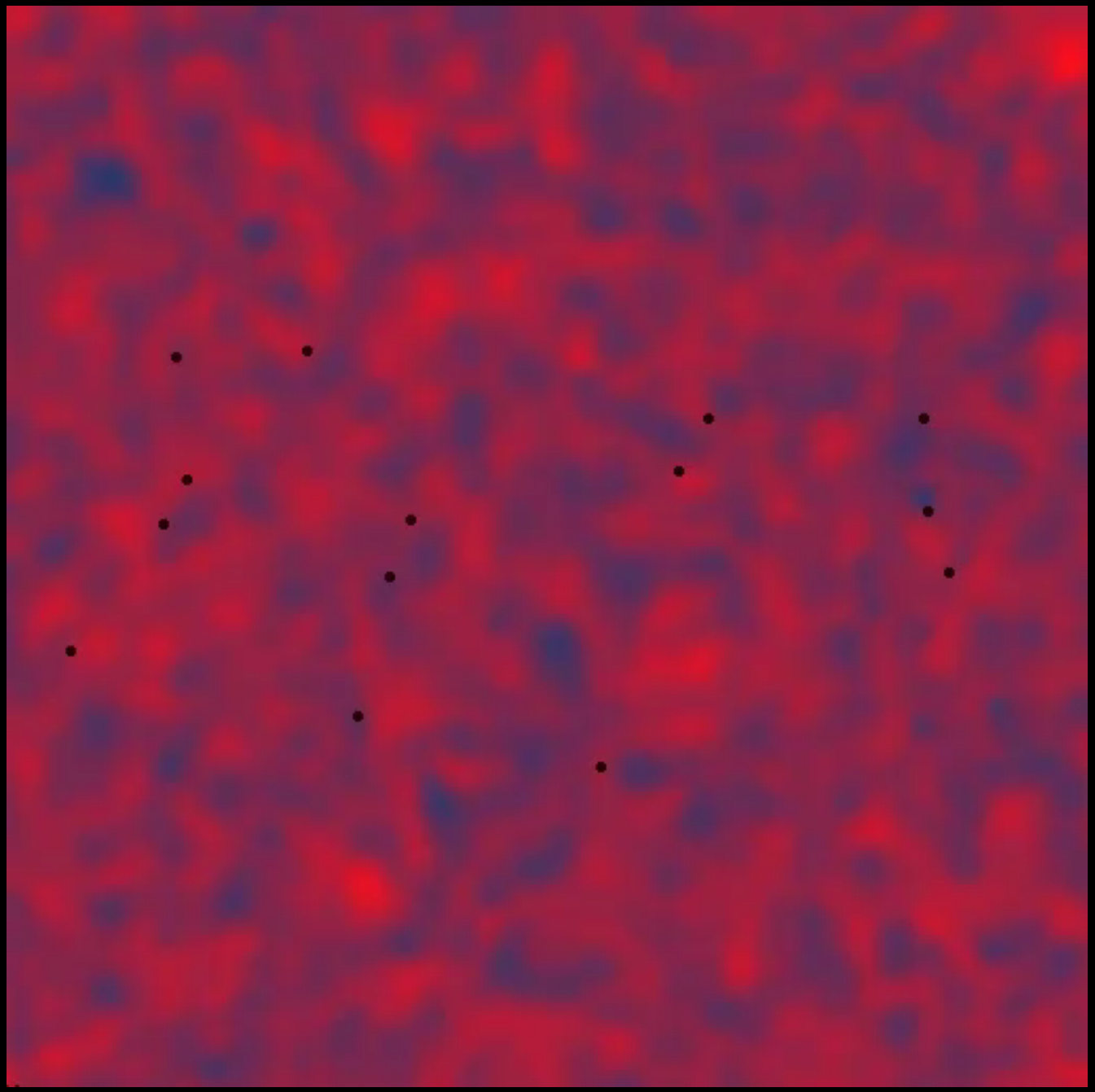

Direct confrontation with the 3-D simulations: imaging

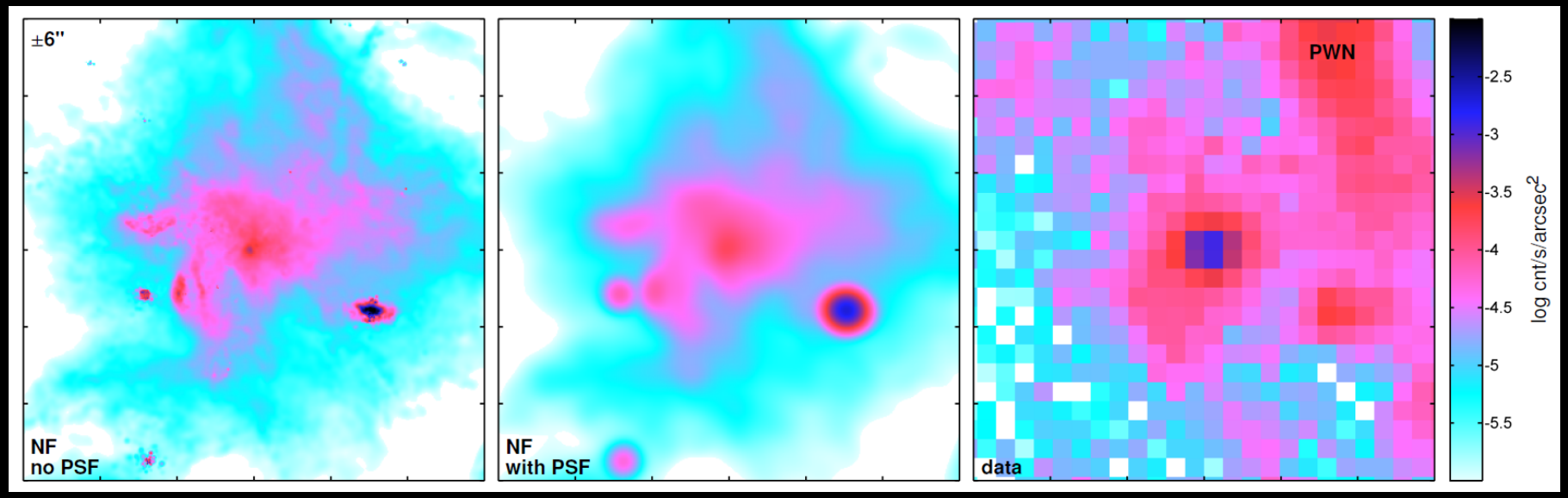

4-9 keV ACIS-S/HETG 0th Order data ±6"

- Abundances: WN8-9 & Ofpe/WN9: CMFGEN models, WN5-7: Onifer+08,WC8-9: Crowther+07
- Response Function Folding and PSF Folding

Russell, Wang, & Cuadra (2016)

X-ray Spectra: Models vs. Data

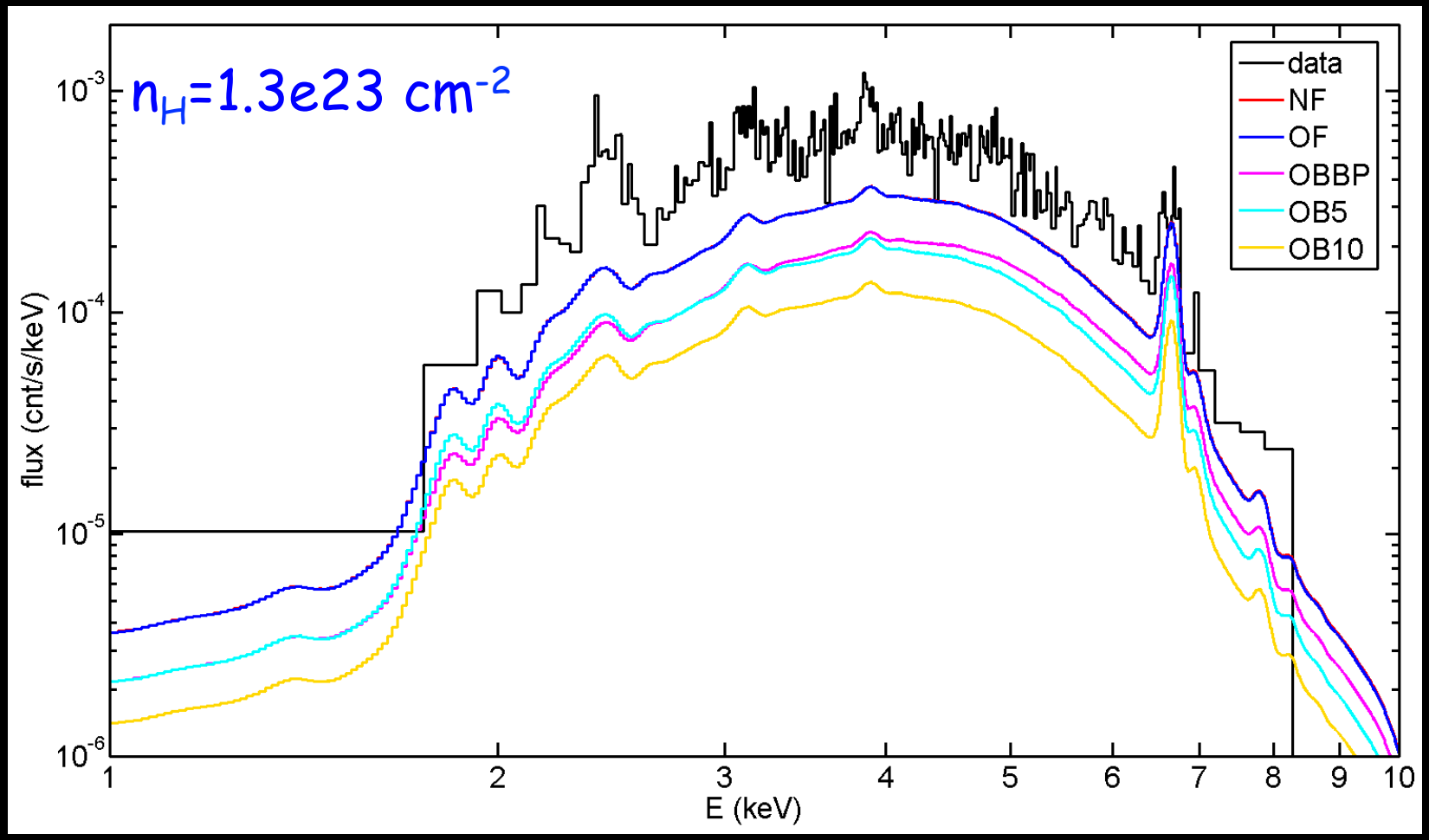

ACIS-S/HETG 0th Order 2″-5″ excluding IRS13E & PWN

X-ray Spectra: Models vs. Data

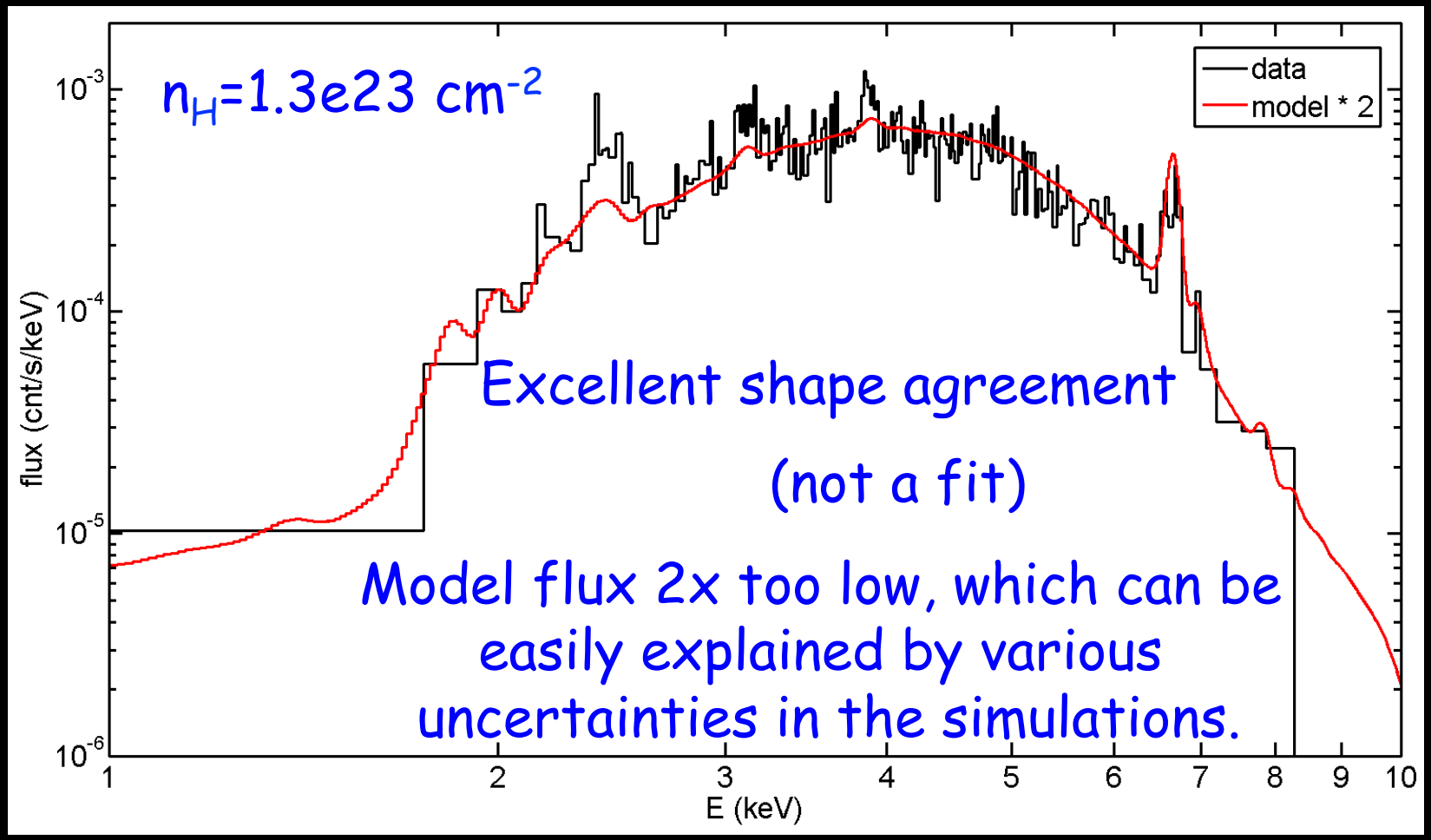

ACIS-S/HETG 0th Order data in the 2"-5" annulus excluding IRS13E & PWN

Summary: 3-D simulations

- 3D Hydro + Radiative Transfer ->
  Model X-ray observation of Galactic center

- Spectral shape: excellent agreement ->
  diffuse emission comes from shocked WR winds

- Flux level: 2x too low
  - Mdot increase of sqrt(2) = 1.4 -> small adjustment
  - Add in O stars & binaries

- Future Work: Improved hydro methods
  - SPH method: "pressure-entropy" (Saithoh&Makino13; Hopkins13)
  - Moving-mesh: GIZMO (Hopkins15)

Interaction of the SMBH with the environment

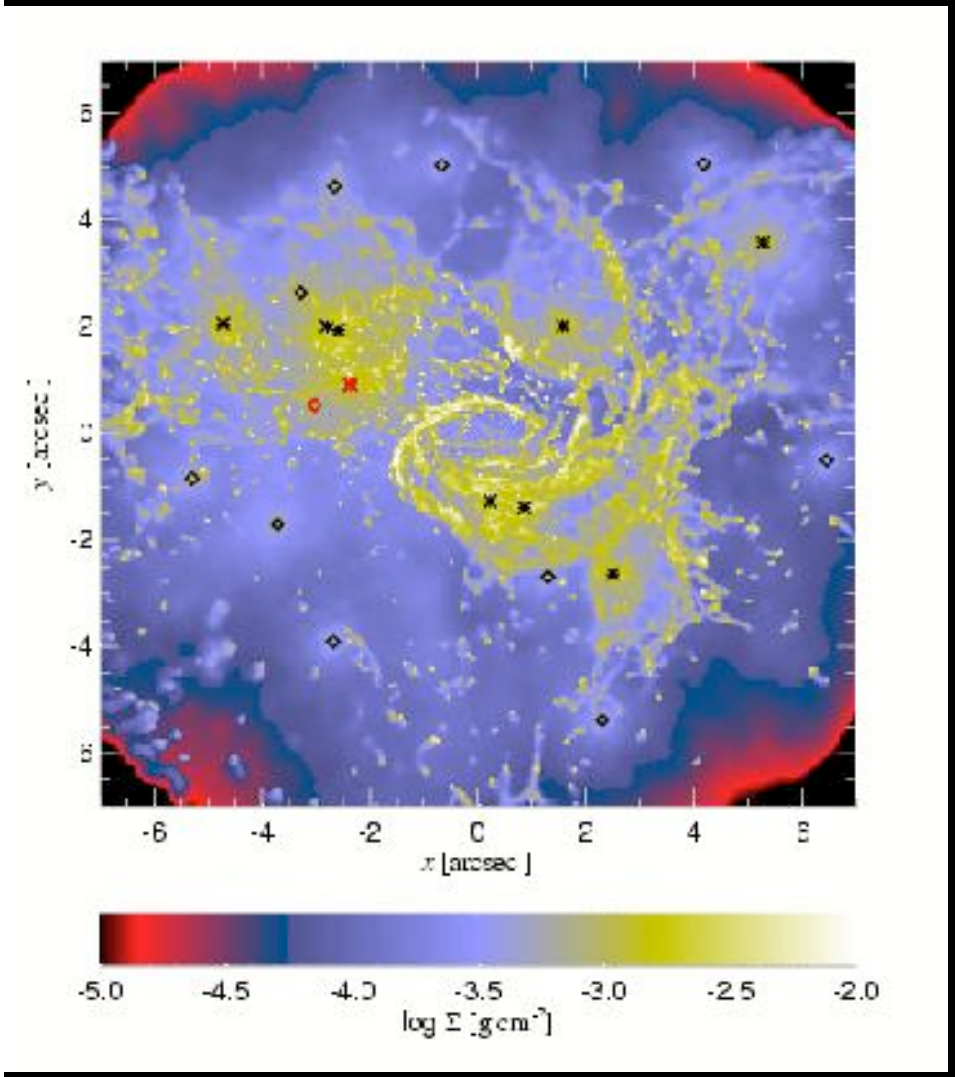

- What is truly responsible for the X-ray emission?
- How does the accretion actually work?
- How does the potential outflow affect the environment? positive or negative feedback?

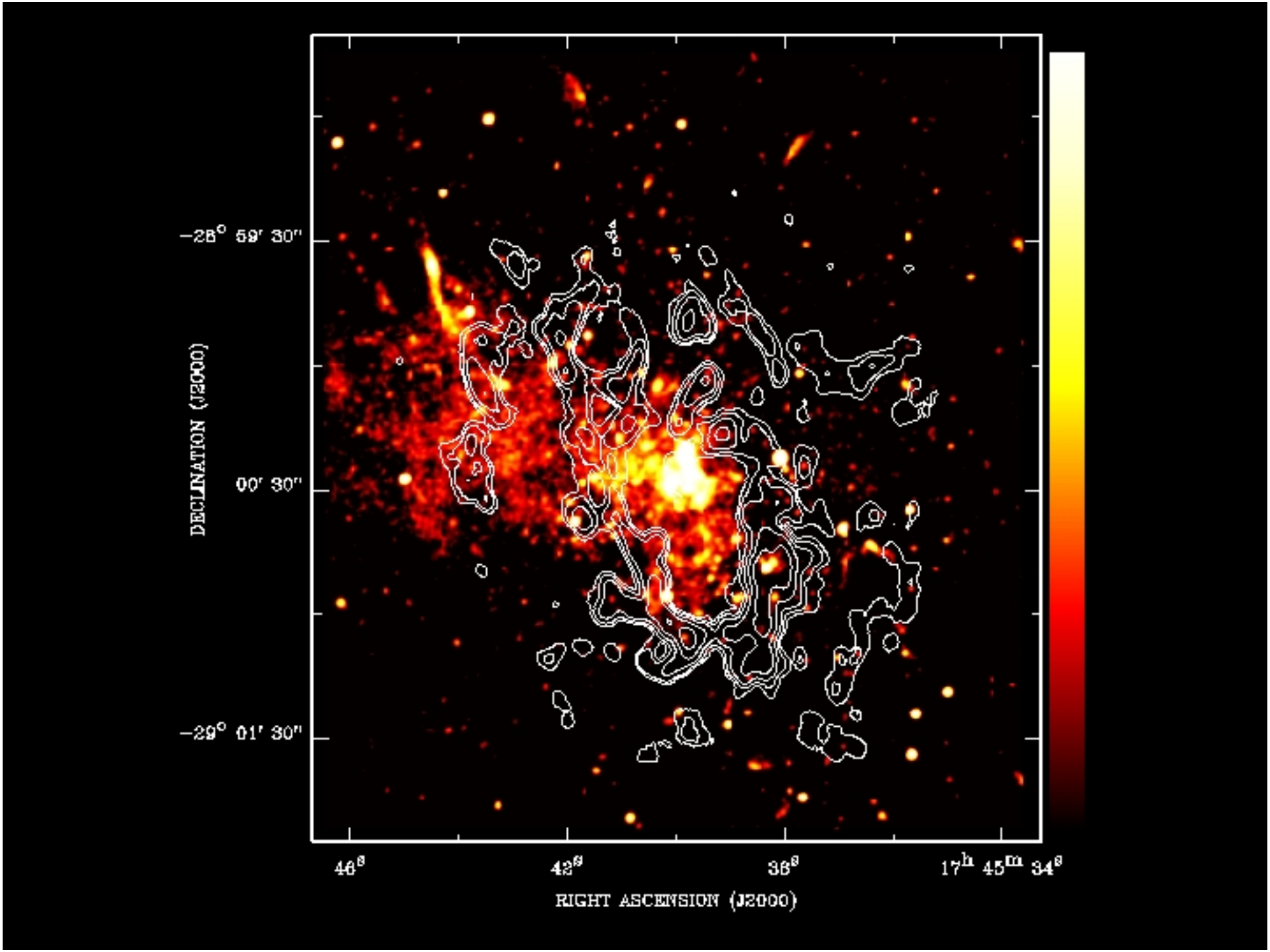
−28° 59′ 30″
00′ 30″
−29° 01′ 30″
DECLINATION (J2000)
46s
42s
38s
17h 45m 34s
RIGHT ASCENSION (J2000)

Time Averaged 2-D Athena Simulations

A set of simulations with different r_c/r_b ratios are performed, which are scalable to cover all the parameter space needed to fit the data.

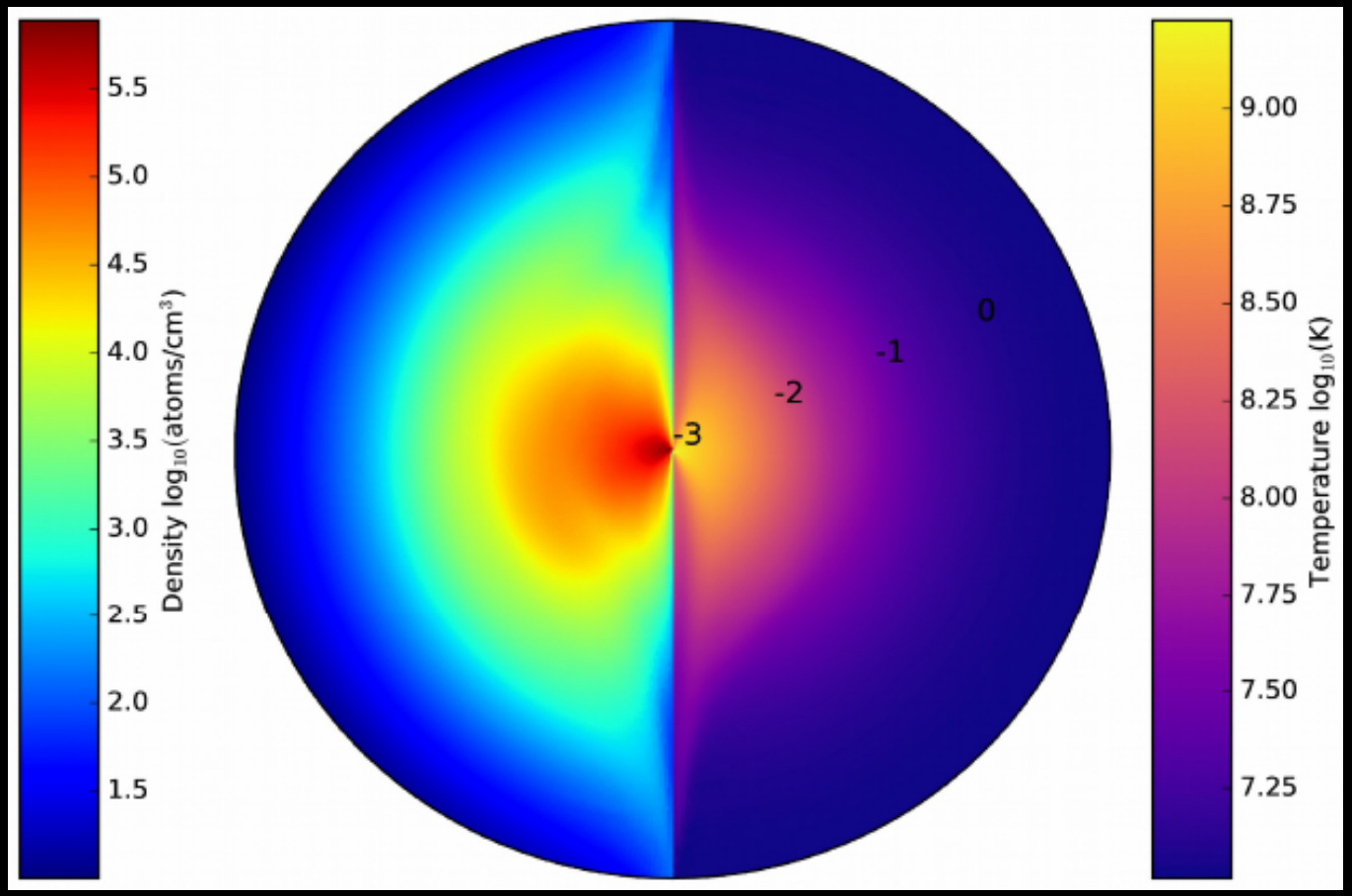

Roberts, Jiang, Wang, & Ostriker (2016)

MCMC hierarchical Bayesian analysis to estimate the top level parameters

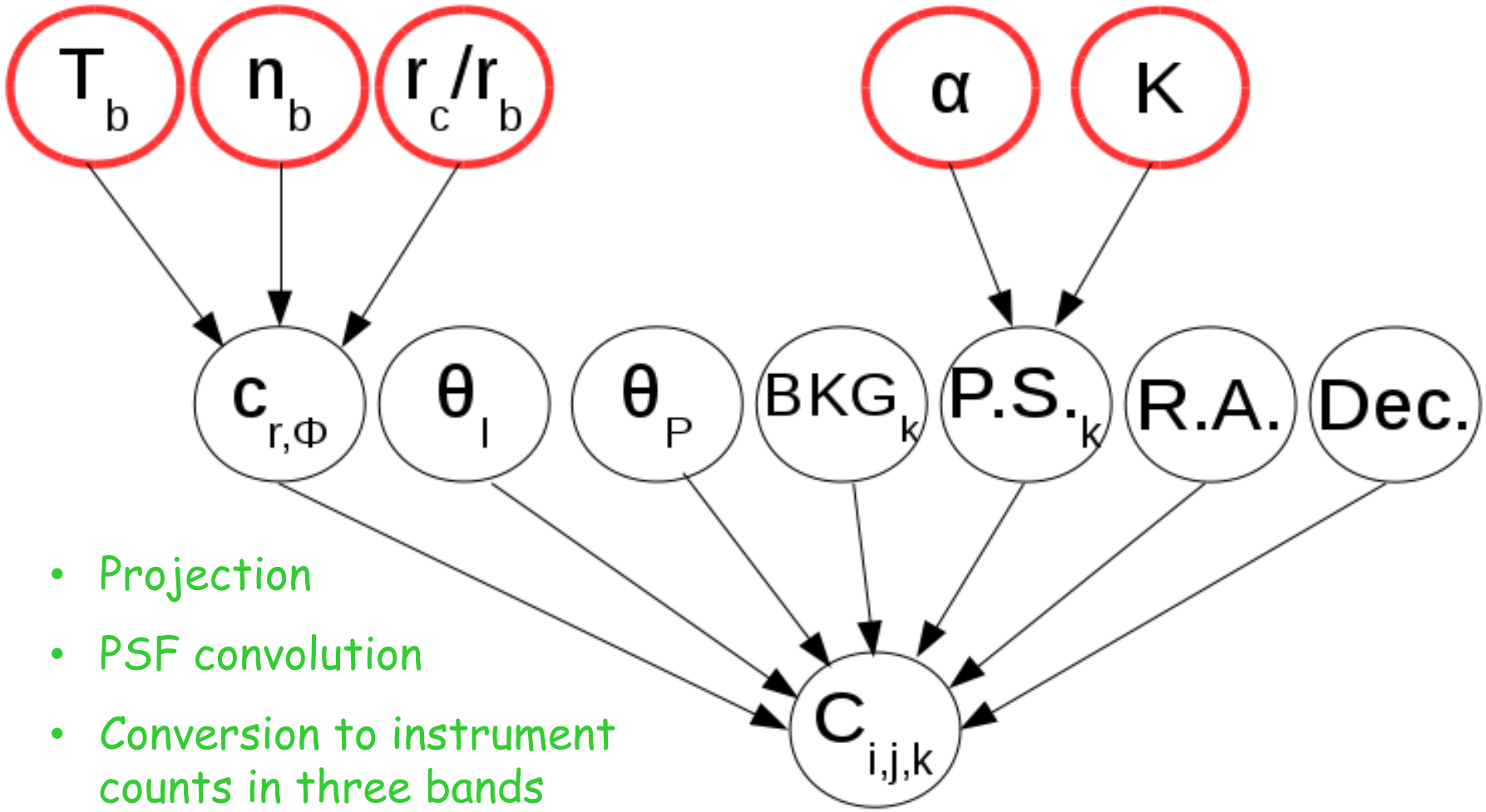

- Projection
- PSF convolution
- Conversion to instrument counts in three bands

Table 2. Summary of the priors. A uniform distribution is represented as U(lower,upper) and a normal distribution is represented as N(mean,sigma).

Parameter	Model	Prior
T_b	All	U(0,inf)
N_b	All	U(0,inf)
r_c/r_b	pBondi-*	0.02 fixed
	All others	U[0.04,0.2]
θ_I	*-wp	N(127,2)
	All others	U[90,180]
θ_P	*-wp	N(99,2)
	All others	U[0,180]
BKG_k	All	U[0,inf)
$P.S._k$	free, pBondi-wp	U[0,inf)
α	*plaw*, dplaw	U[1,10]
K	*plaw*, dplaw	U[0,inf)
α_{flare}	dplaw	N(2.6,0.12)
K_{flare}	dplaw	U[0,inf)

Best-fit model, data, and residual images

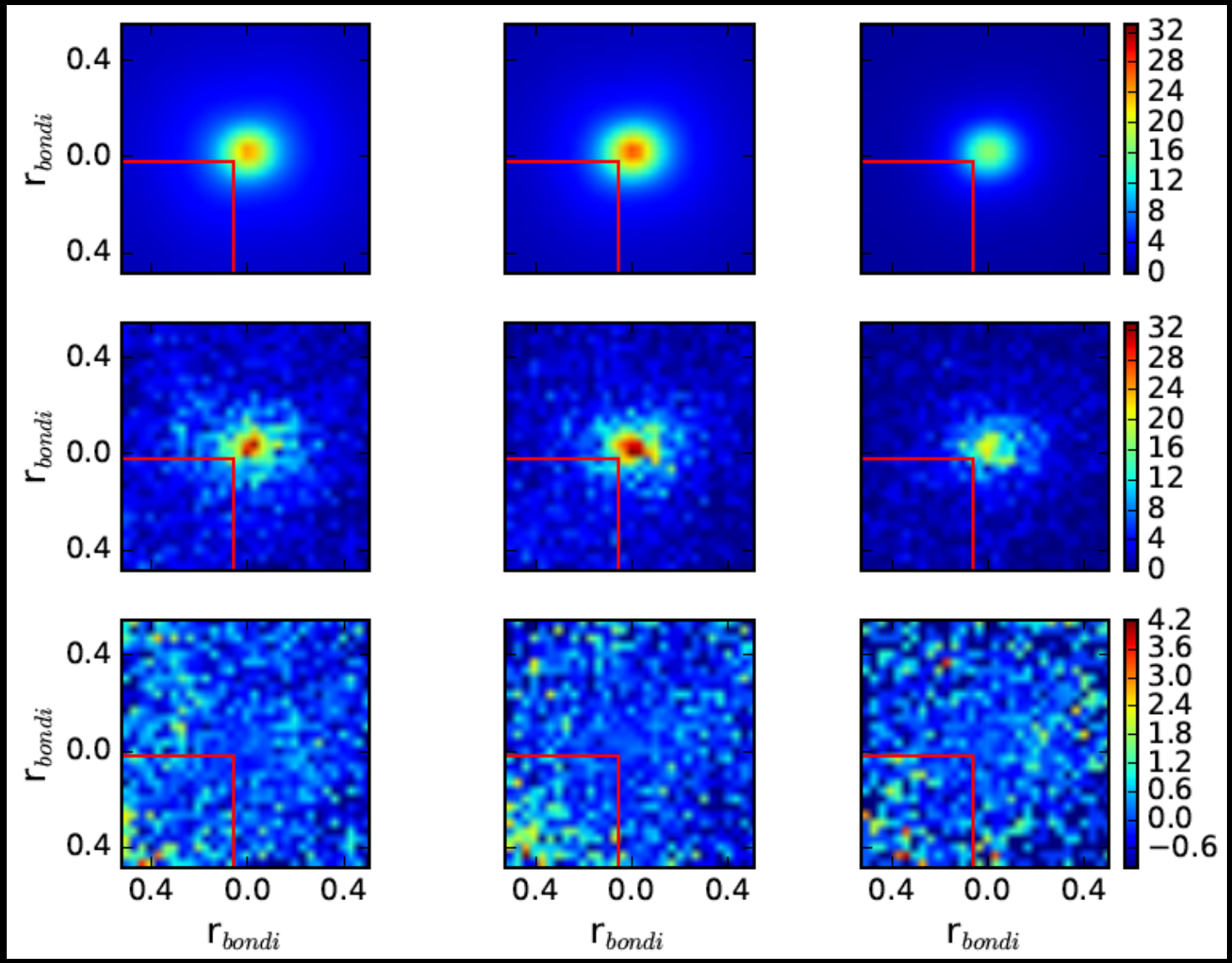

1-4 keV 4-5.5 keV 5.5-9 keV

Best fit and 1σ confidence intervals of free parameters

θ_I (deg.)	126.4 (125.0,127.7)
θ_P (deg.)	99.1 (97.8,100.5)
r_c/r_b	0.058 (0.052,0.064)
T_b (K)	1.30e7 (1.24e7,1.38e7)
n_b (cm^{-3})	187.0 (174.9,197.6)
BKG1 (counts/pix)	0.14 (0.03,0.32)
BKG2 (counts/pix)	0.39 (0.25,0.53)
BKG3 (counts/pix)	0.52 (0.39,0.61)
α	4.95 (3.96,6.76)
$\log_{10}(N)$	2.69 (2.18,3.63)

The orientation of the accretion flow is consistent with so-called clockwise stellar disk.

Flow parameters

T_b: 1.30e7(±0.06e7) K n_b: 187 (±11) cm^{-3} r_c/r_b: 0.058 (±0.006)

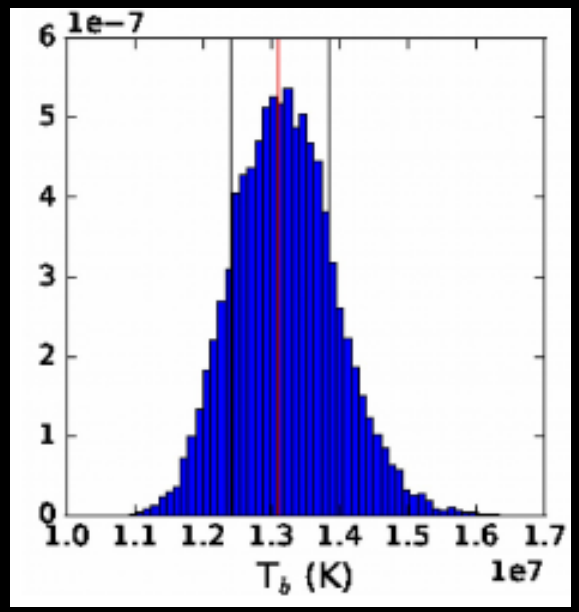

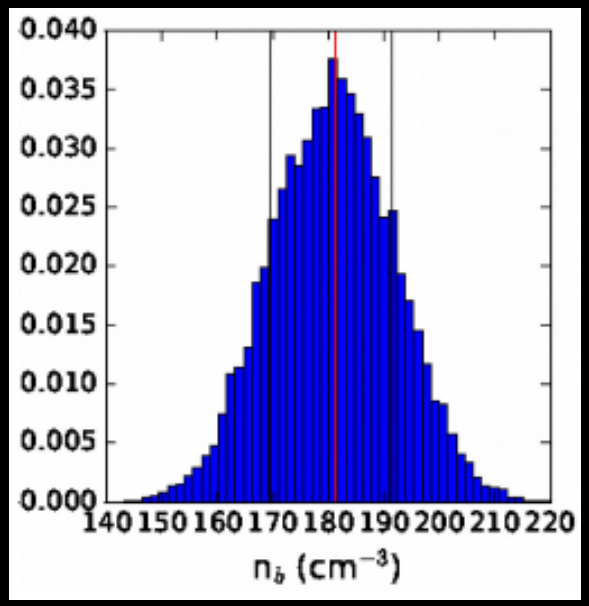

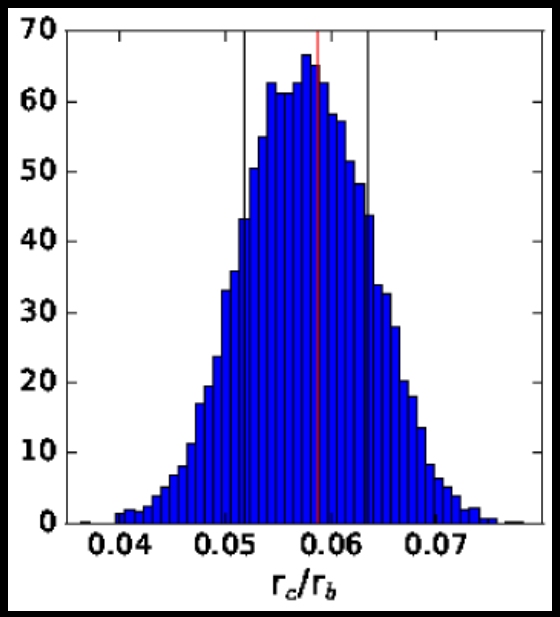

- Consistent with a shocked stellar wind origin.
- 1st direct estimate of the circularization radius --- an angular momentum characterization.

Angular momentum flattens the density profile of the flow

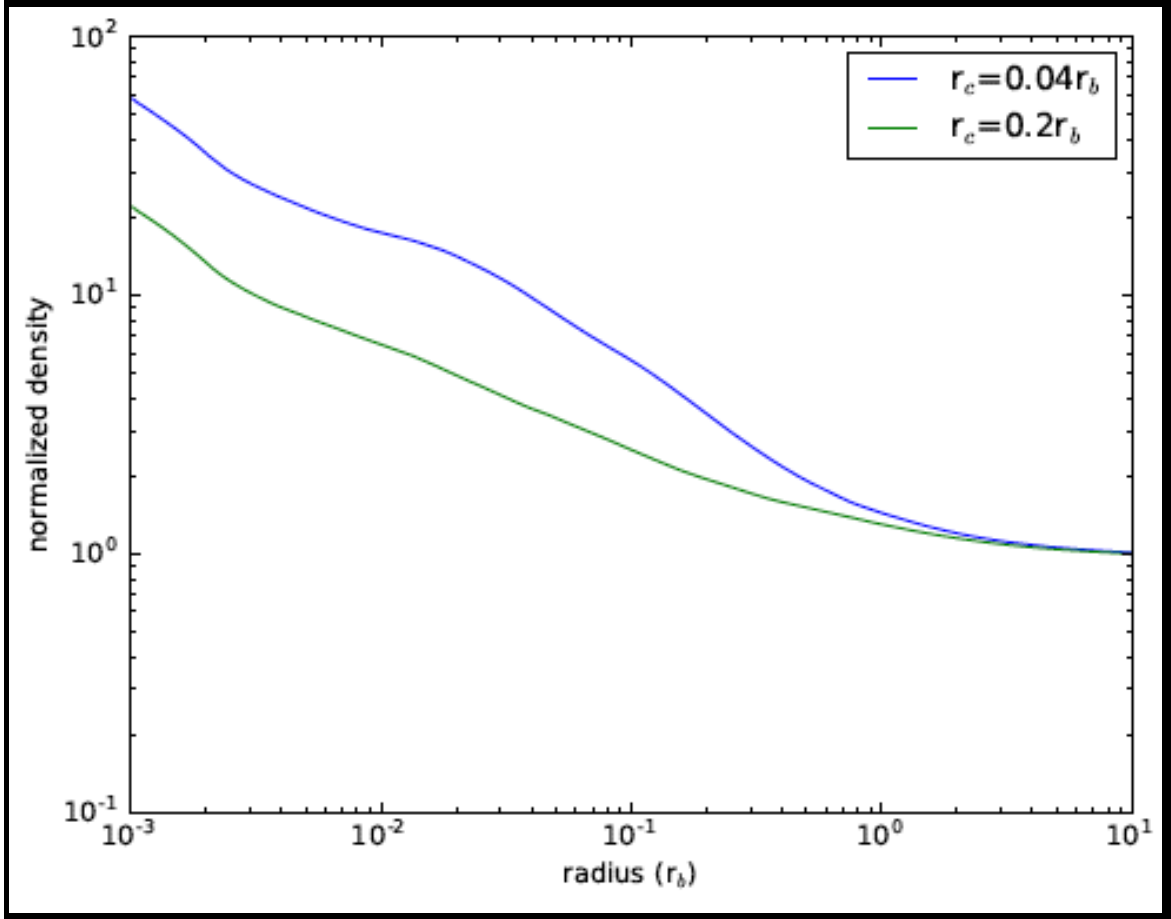

The different profiles give different predictions of the X-ray spectrum and the outflow pattern and energetics.

Normalized azimuthally averaged density profiles for two differerent simulations.

Point-like Source

- 5.8% of the emission arises the unresolved point-like emission inside the inner boundary of the simulation (< 10^2 r_s).
- Emission possibilities:
  - Bremsstrahlung (accretion f[illegible])
  - S[illegible] (unresolved flares)
  - Inverse-Compton (low energy synchrotron scattered by the hot electrons)

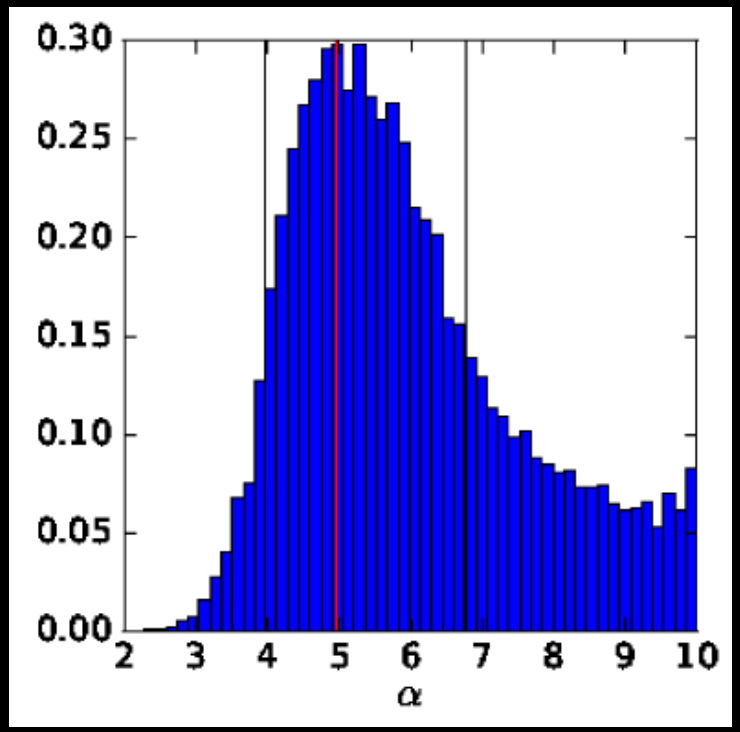

Bursts and accretion flow onset

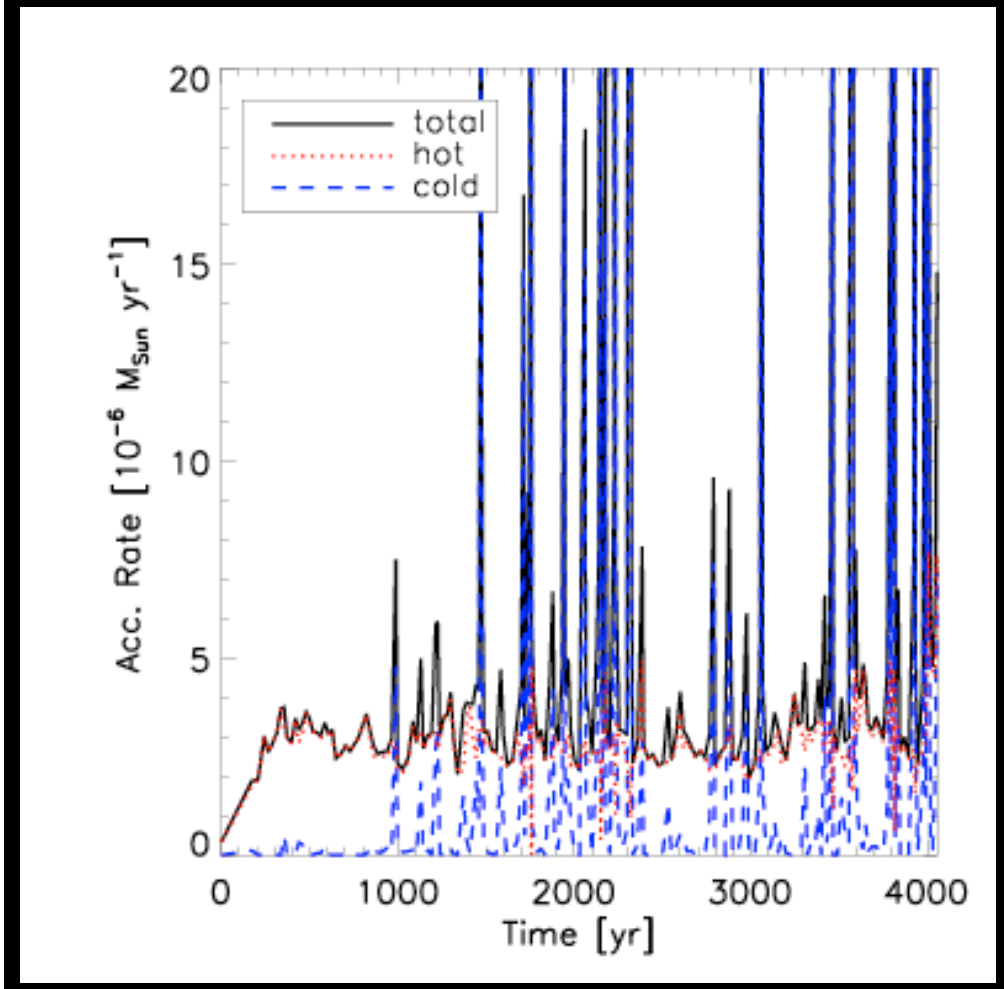

Cuadra et al (2006)

- Various bursts are expected on roughly 10^2 yr time scales.
- Such a burst may sweep away much of the hot accretion flow, which would then need to be re-established.
- The current X-ray size of Sgr A*, ~ 1.5" radius, may represent such an onset of the flow since the last burst ~10^2 yrs ago.

How does activity of the SMBH vary with time?

- What are the frequency and durations of bursting episodes?
- Why is such question important?
  - the correlation between SF and AGN.
  - the understanding of the state of the ISM, CGM, and the surrounding IGM.
- How can the question be addressed?
  - Reflection light
  - Non-ionization equilibrium state of the gas

X-ray reverberation: Sgr A* burst ~ 100-300 years ago

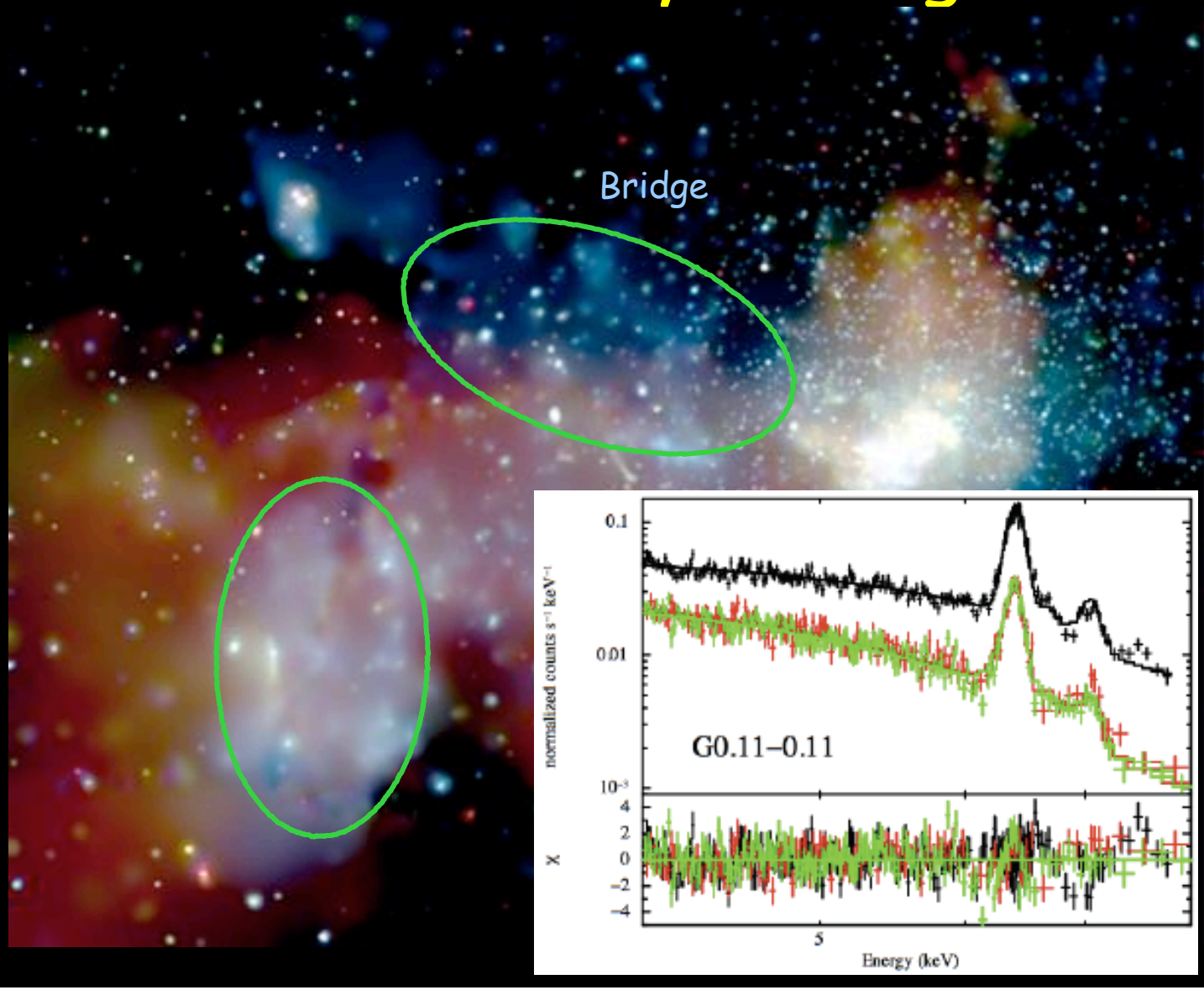

X-ray reverberation of a Sgr A* burst ~ 100 years ago

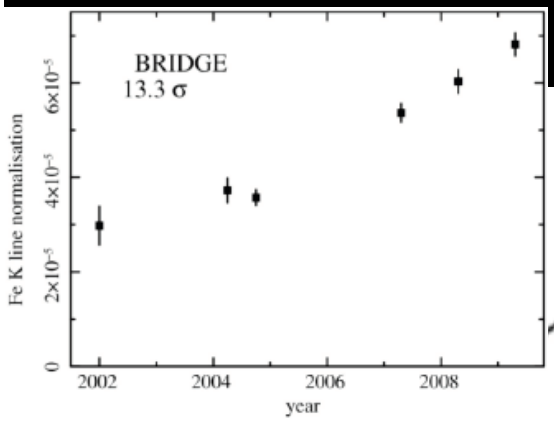

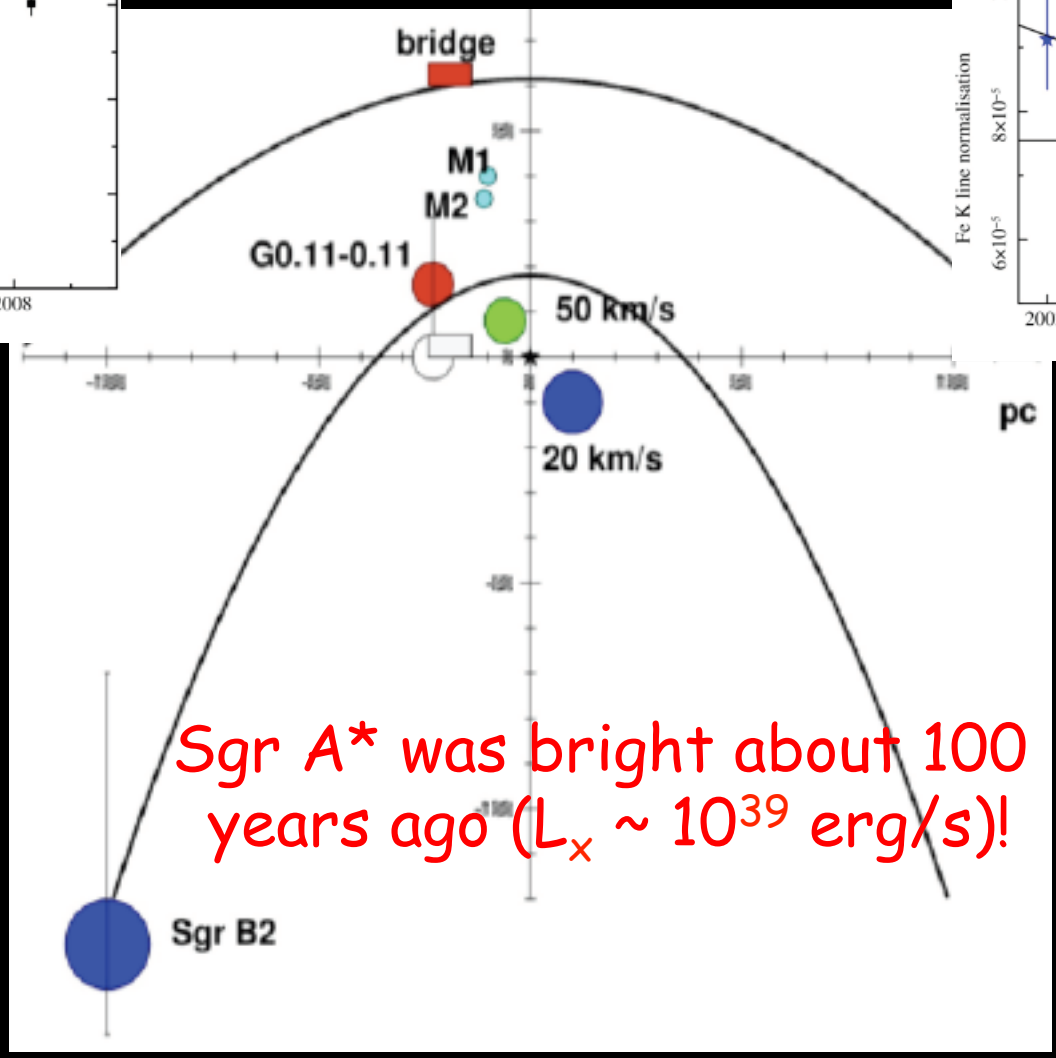

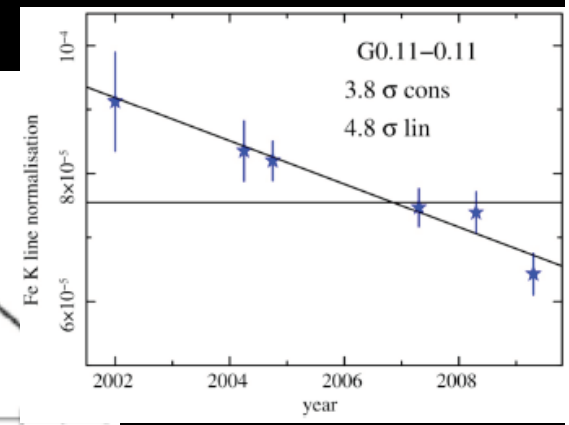

Sgr A* was bright about 100 years ago (L_x ~ 10^{39} erg/s)!

The largest uncertainty is in the line-of-sight locations of the clouds!

Ponti et al. 2010

The Large Millimeter Telescope

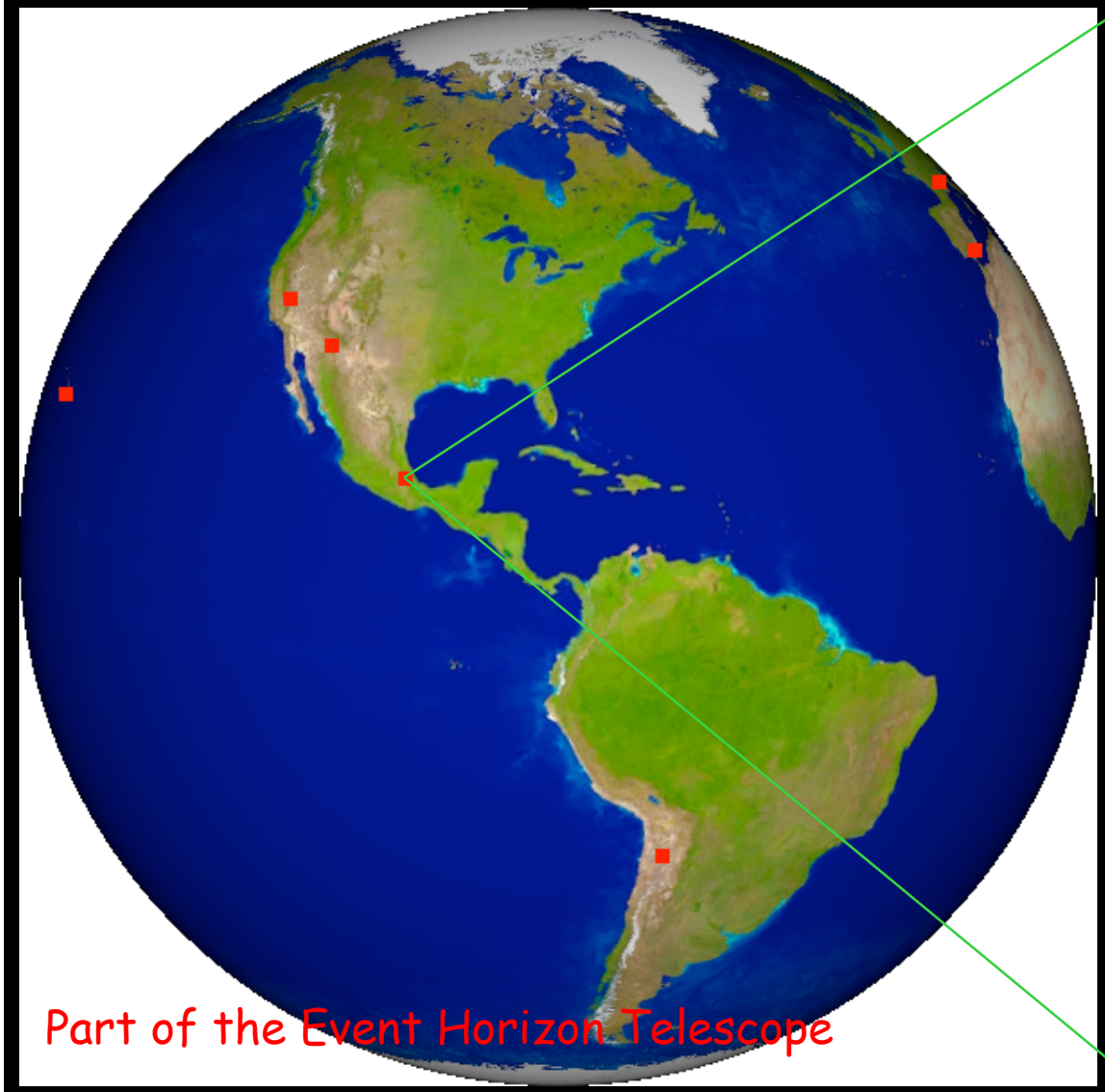

Only 32 m diameter is ready currently. AzTEC and RSR have been fully commissioned.

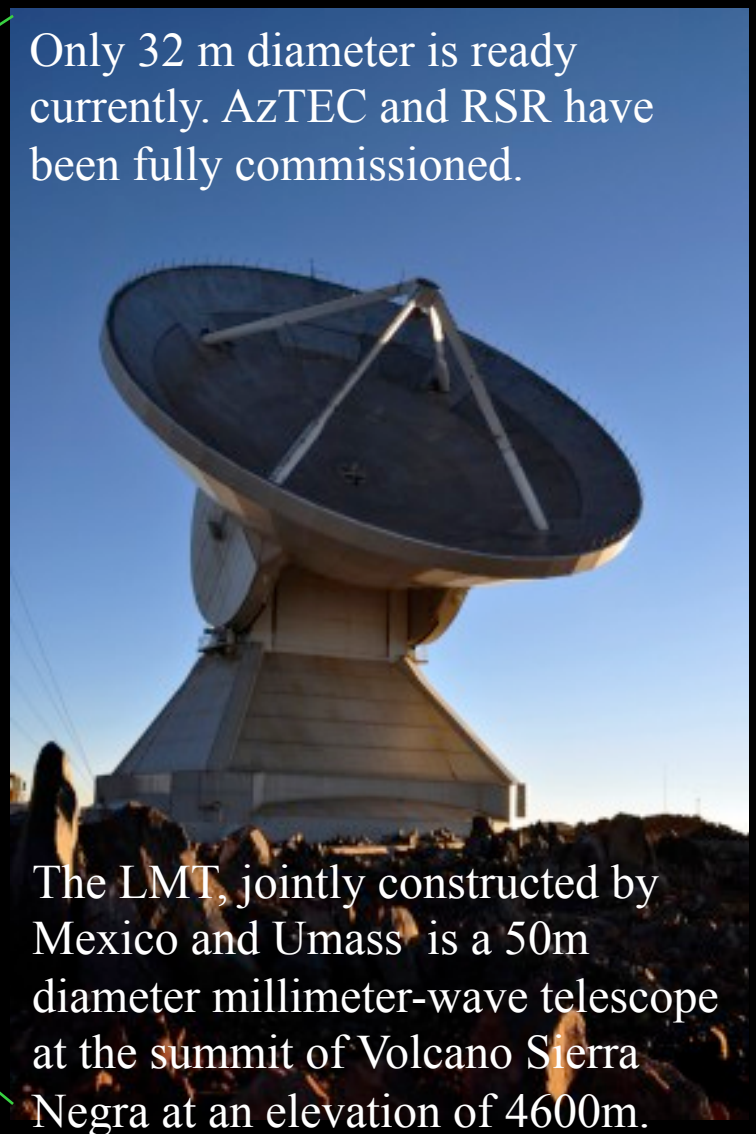

The LMT, jointly constructed by Mexico and Umass is a 50m diameter millimeter-wave telescope at the summit of Volcano Sierra Negra at an elevation of 4600m.

LMT/AzTEC 1-mm map of the CMZ

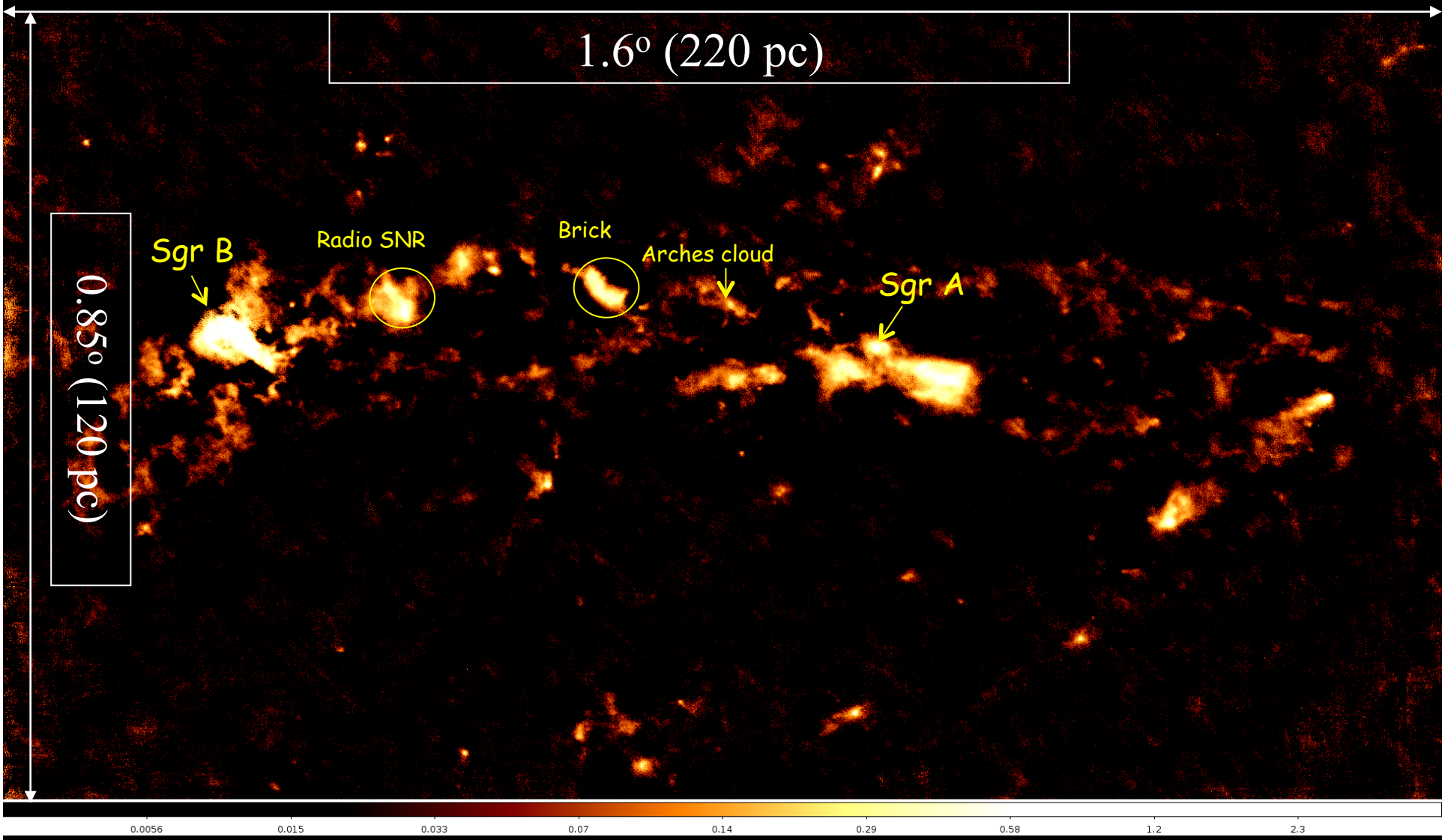

1.1-mm composite map of the CMZ

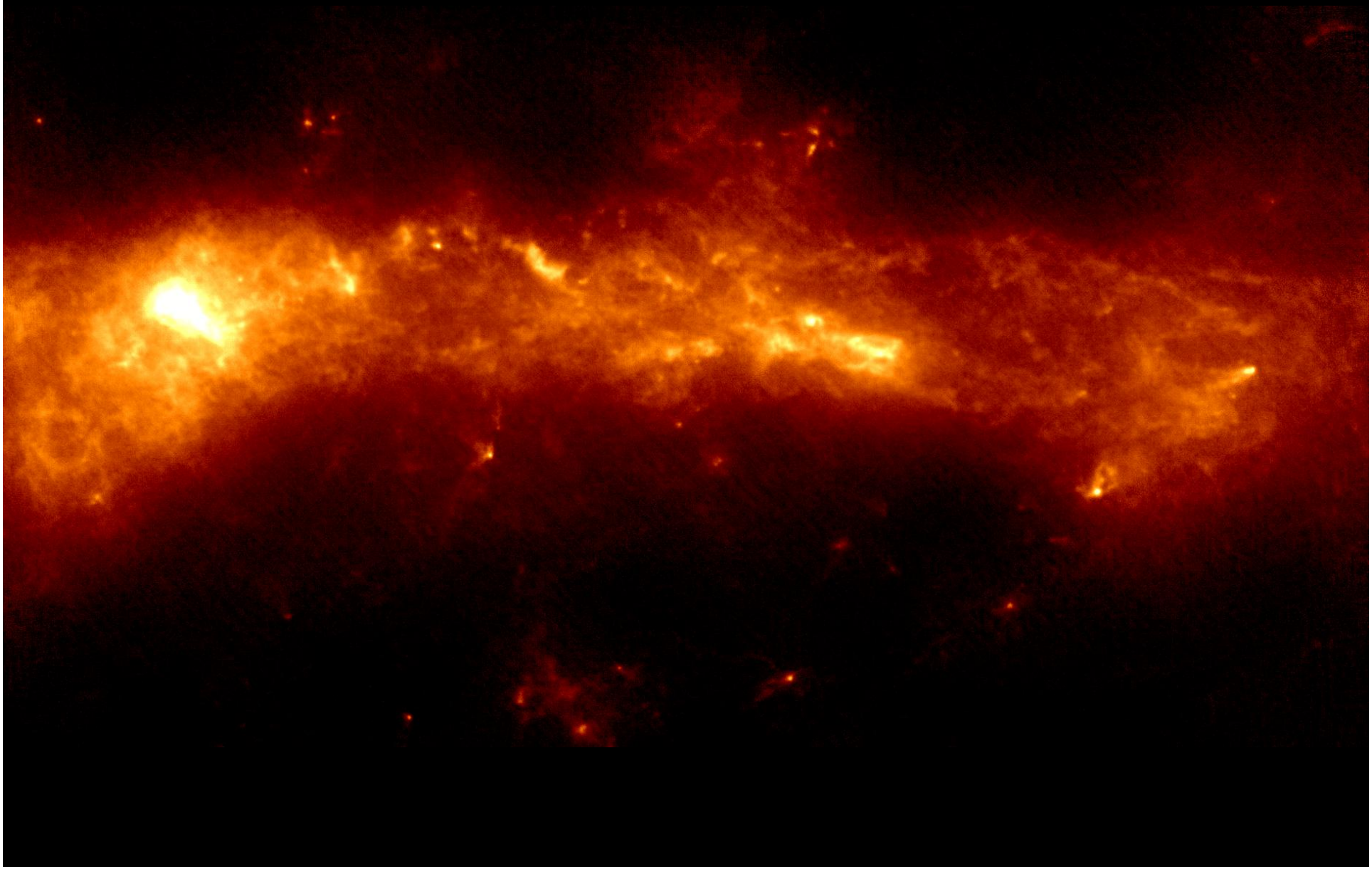

Multiwavelength dust map of the CMZ

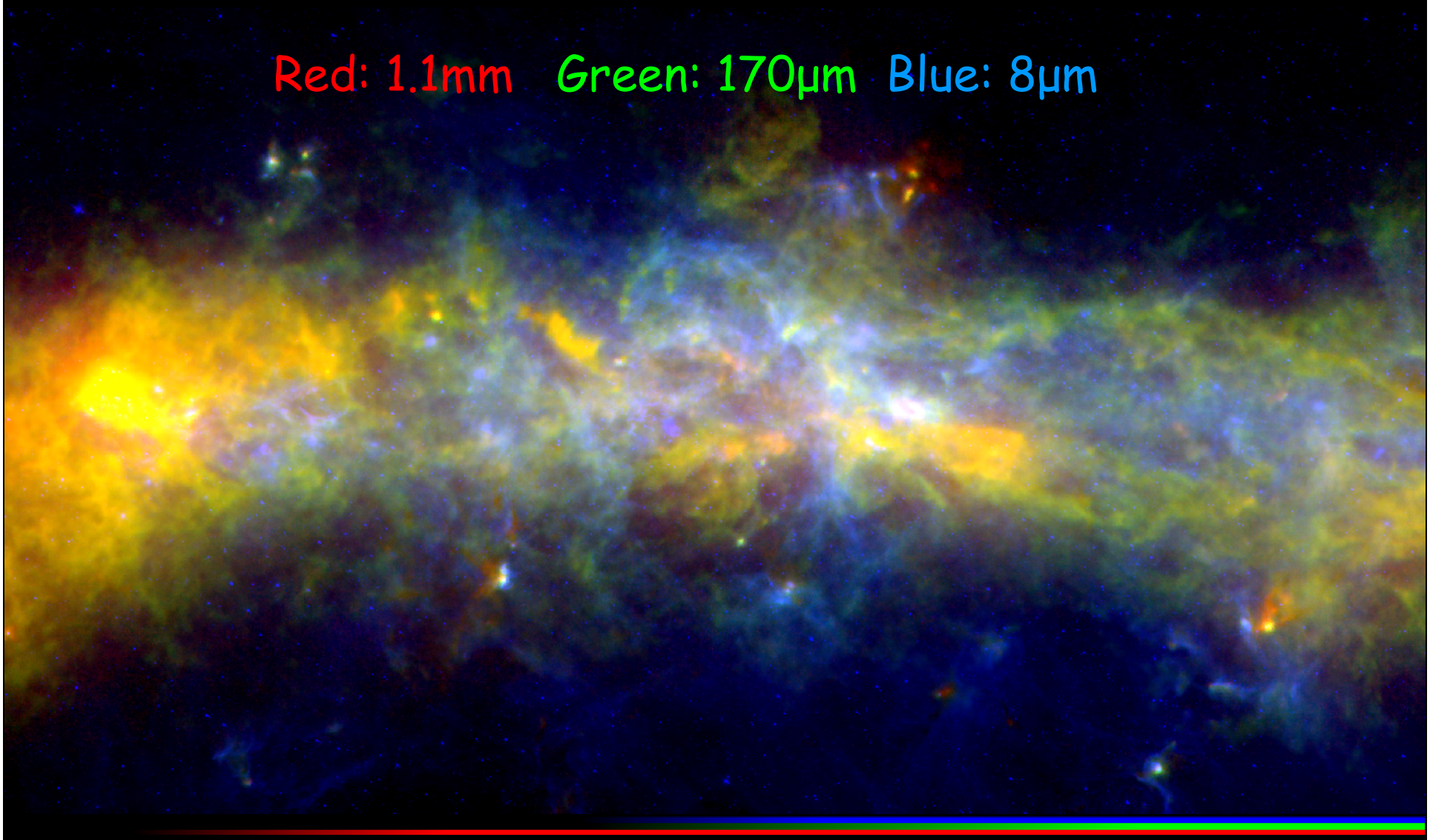

Earlier Galactic center activity? Detection of recombining plasma.

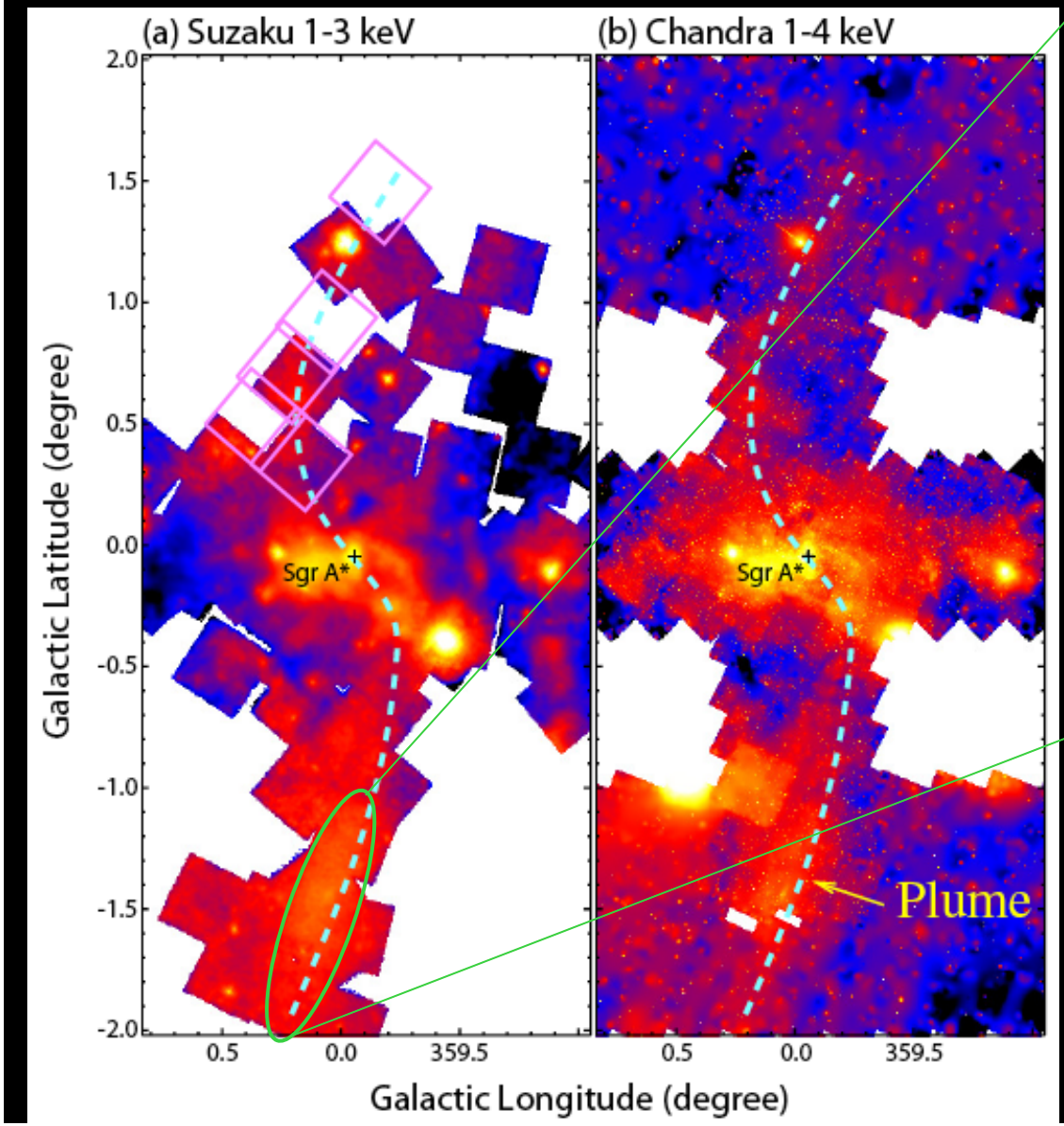

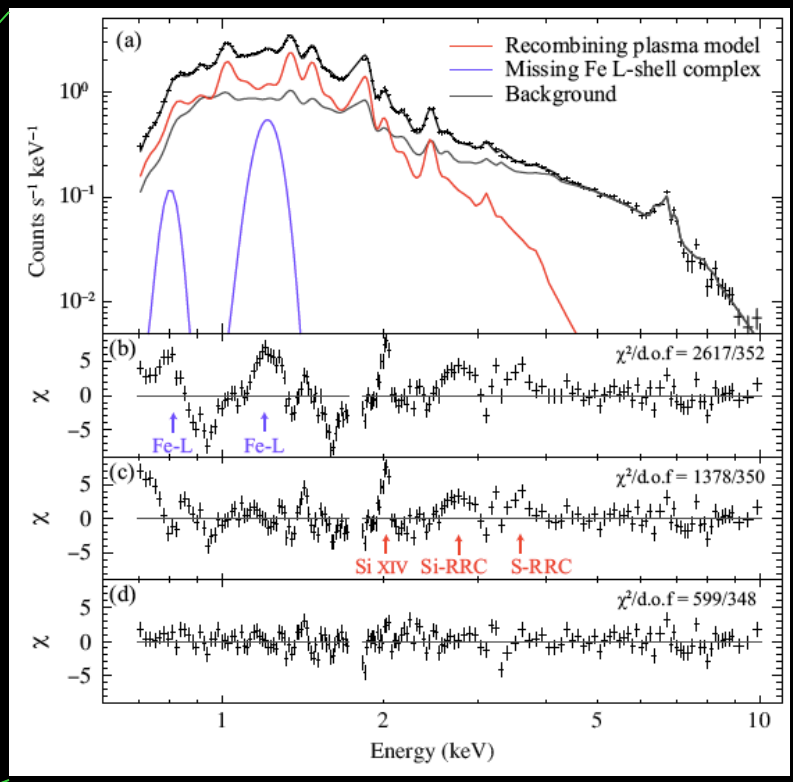

S. Nakashima et al. 2013

Fermi Bubble: a relic of even earlier nuclear activities?

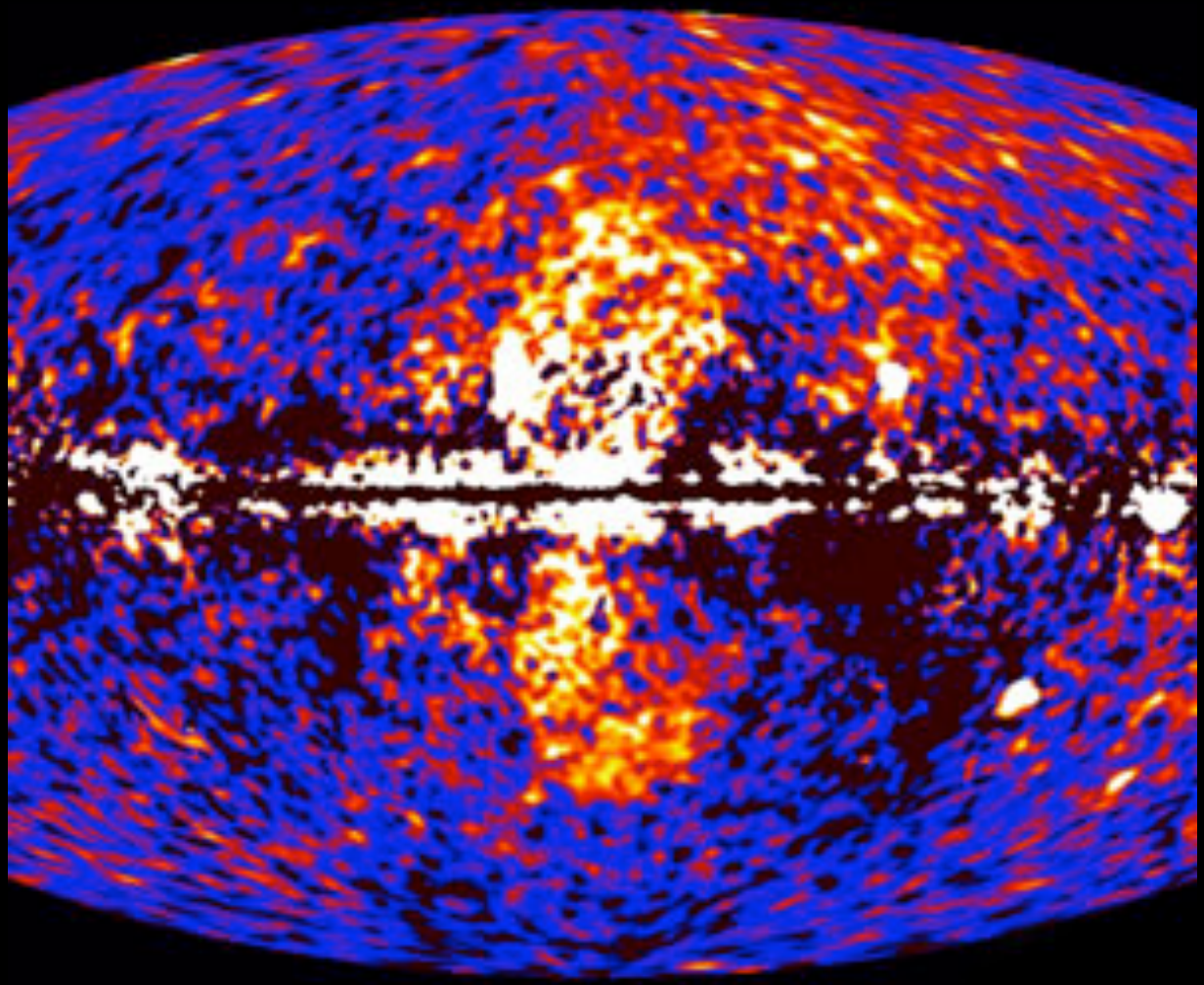

- Bipolar morphology on ~10 kpc scale.
- Possible energy source of ~10^{55} ergs injected from the GC ~10^{7} years ago.

Su et al. (2010)

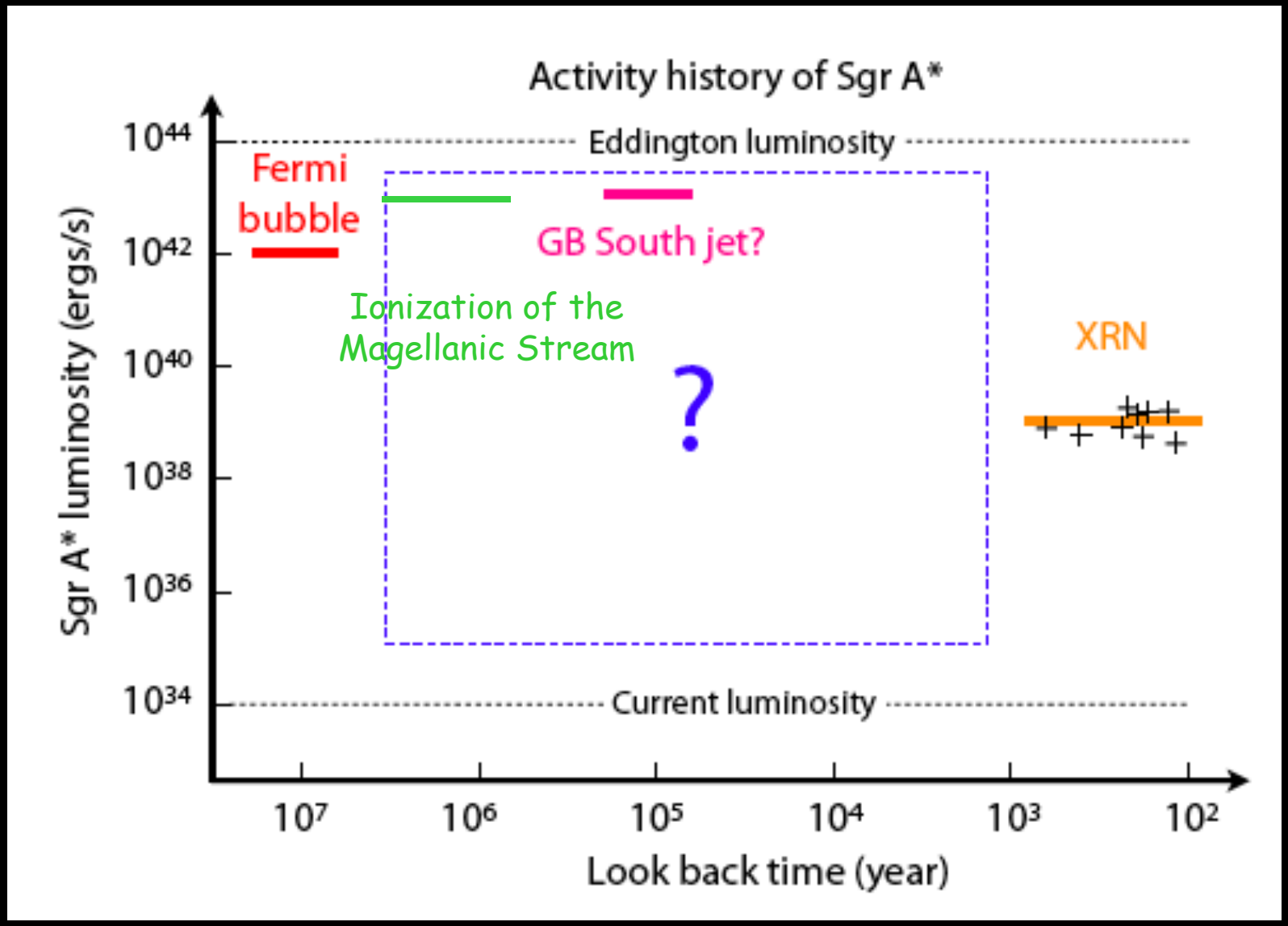

Bland-Hawthorn et al. (2013)

Summary

- The shocked stellar wind scenario for the accretion is confirmed, especially by the temperature and density at the Bondi radius.
- We have made the first direct estimates of the inclination angle and circularization radius (~0.058 r_b) of the accretion flow, providing a needed constraint for theoretical models.
- The unresolved point-like emission is primarily produced through Inverse Compton scattering of low energy synchrotron emission by the hot thermal plasma near the BH.
- Detailed 3-D MHD simulations can now be carried out for further testing of the theory, confronting such observations as Faraday's rotation measurements.
- More can be learned about the recent burst history of Sgr A*, based on the 3-D distribution measurement of the dense dusty clouds, as well as the non-equilibrium modeling the diffuses X-ray emission.

Gracias por su atención!

X-ray flare detection: method and results

- Maximum likelihood fitting to the X-ray data with unbinned Cash statistics, assuming Gaussian flares.
- Pileup applied to the expected lightcurve.
- MCMC algorithm to better characterize the measurement of parameter uncertainties.
- 33 flares in 46 ACIS-I observations from 1999 to 2001, and 49 flares in 39 ACIS-S observations with high energy transmission gratings in 2012.

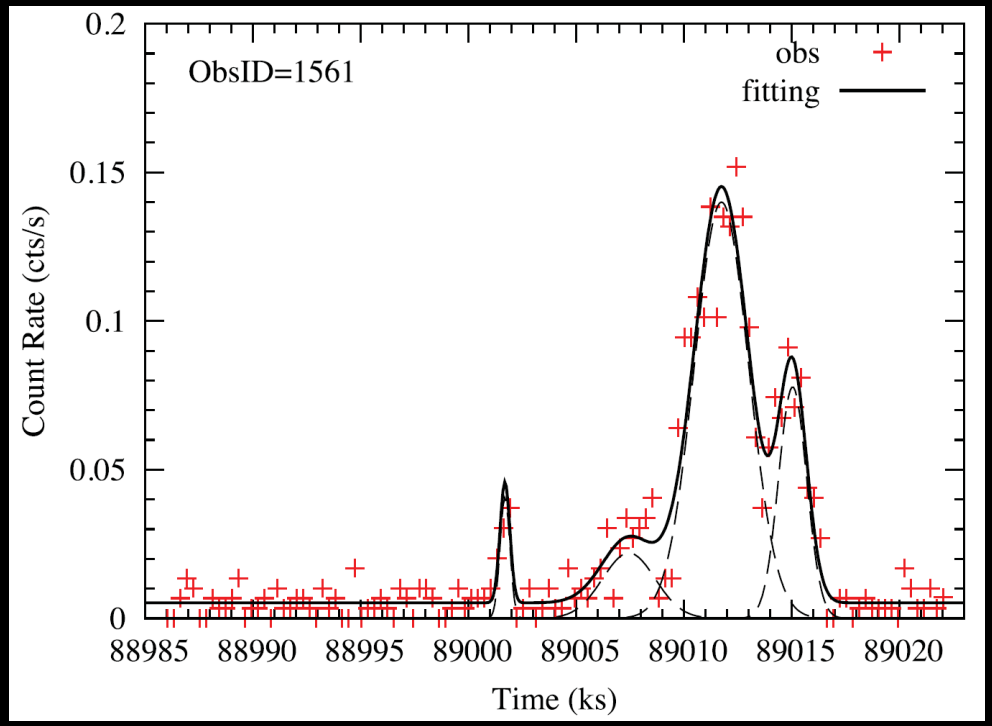

Yuan & Wang (2016)

Improvements over previous work

- First measurements of duration errors
- More complete sample close to detection limit

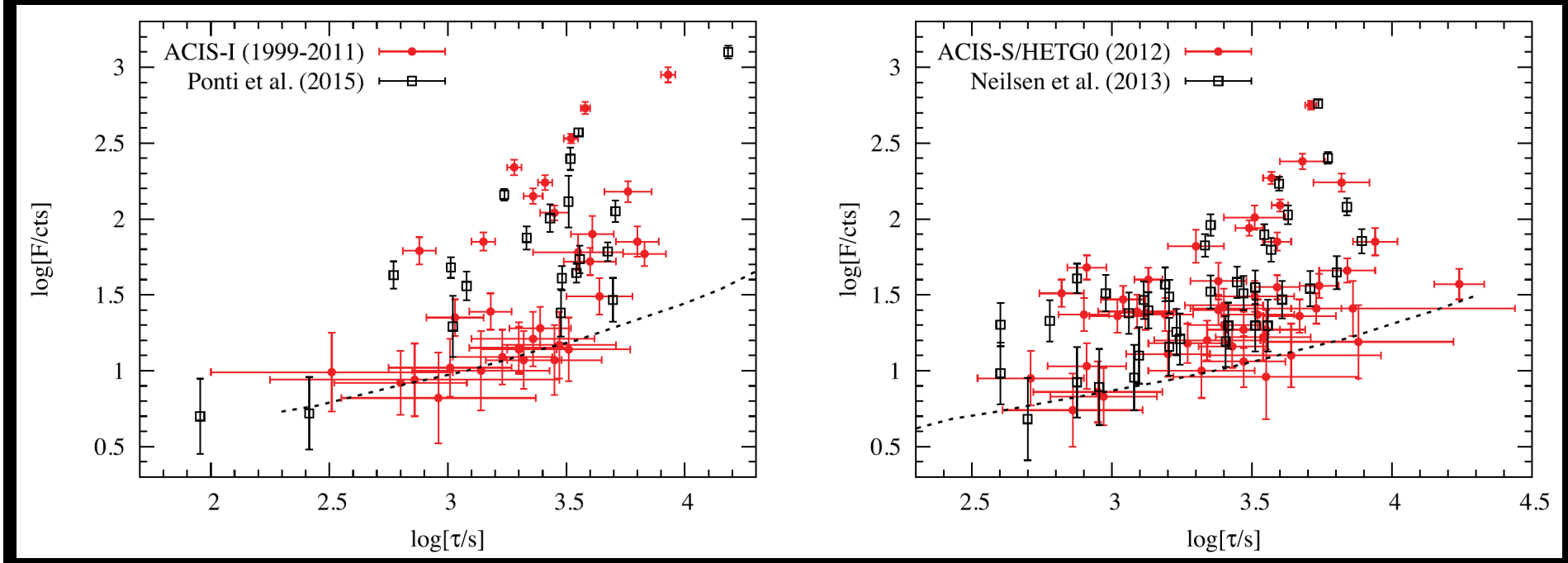

Fluence versus duration distributions of the detected flares for the ACIS-I (left) and -S (right) observations, compared to those of Ponti et al. (2015) and Neilsen et al. (2013).

"Quiescent" emission shows no systematic change during or after G1/S2's pericenter passages

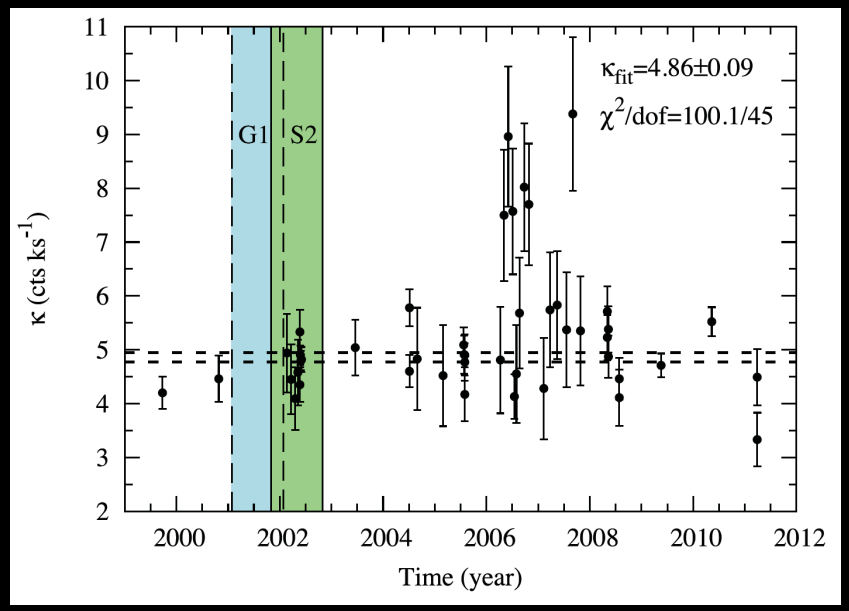

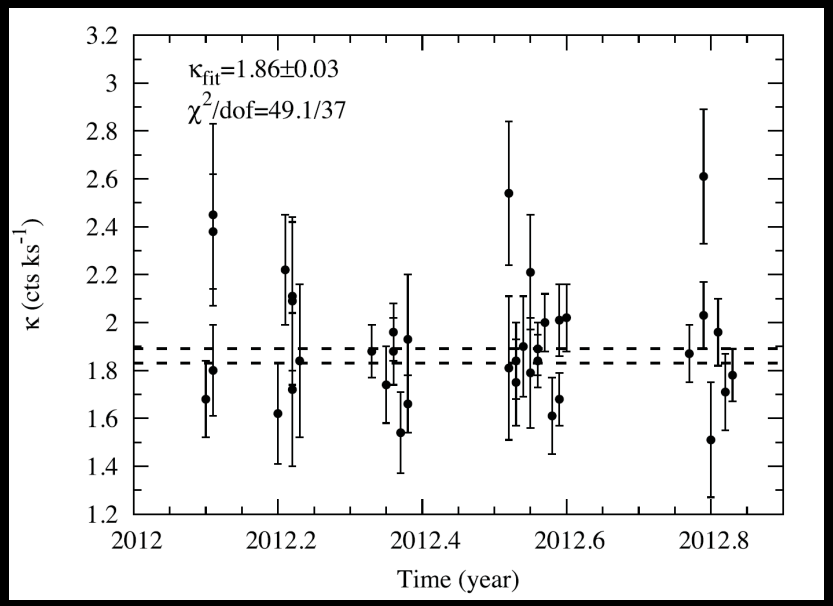

- ACIS-I (2000-2012) total 1.4 Ms
- Constant fitting:
- CNRT=3.98+/-0.09
- χ^2/dof~100.7/43
- Intrinsic RMS < 15

- ACIS-S (2012) total 3 Ms
- Constant fitting
- CNRT=2.35+/-0.03
- χ^2/dof~39.9/37
- Intrinsic RMS < 3%

Yuan & Wang 2016

No significant change in the flare rate

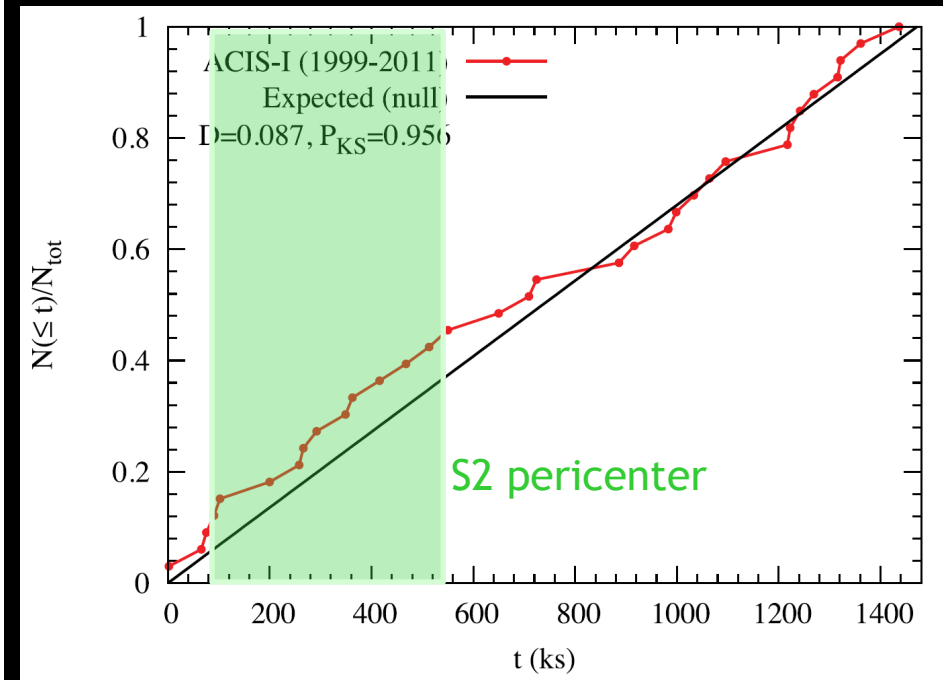

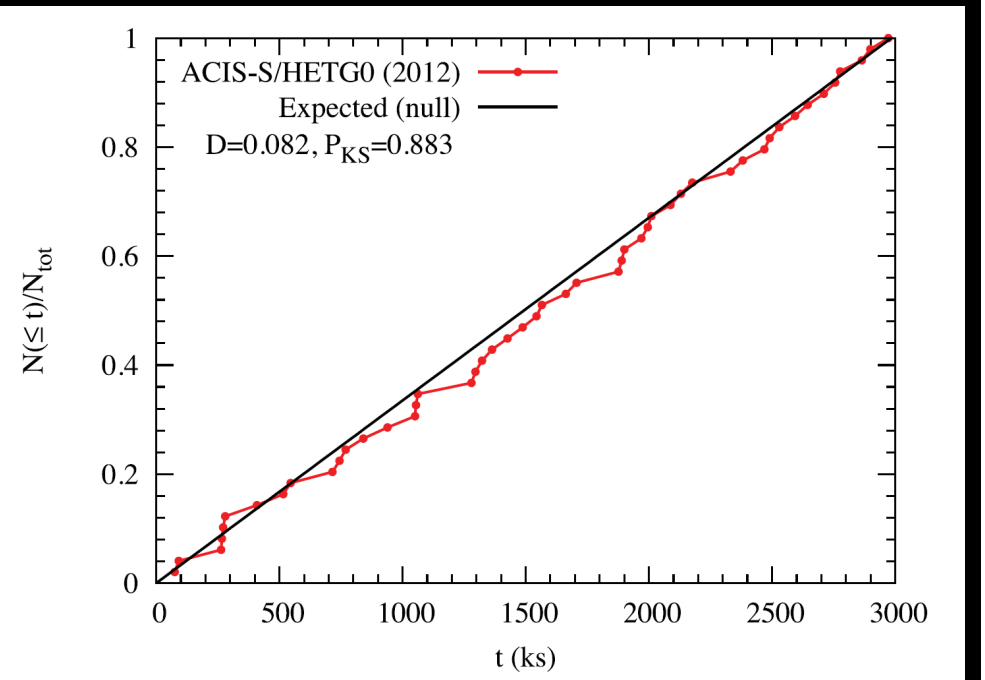

Evidence for short-term clustering of the flares at ~40 ks

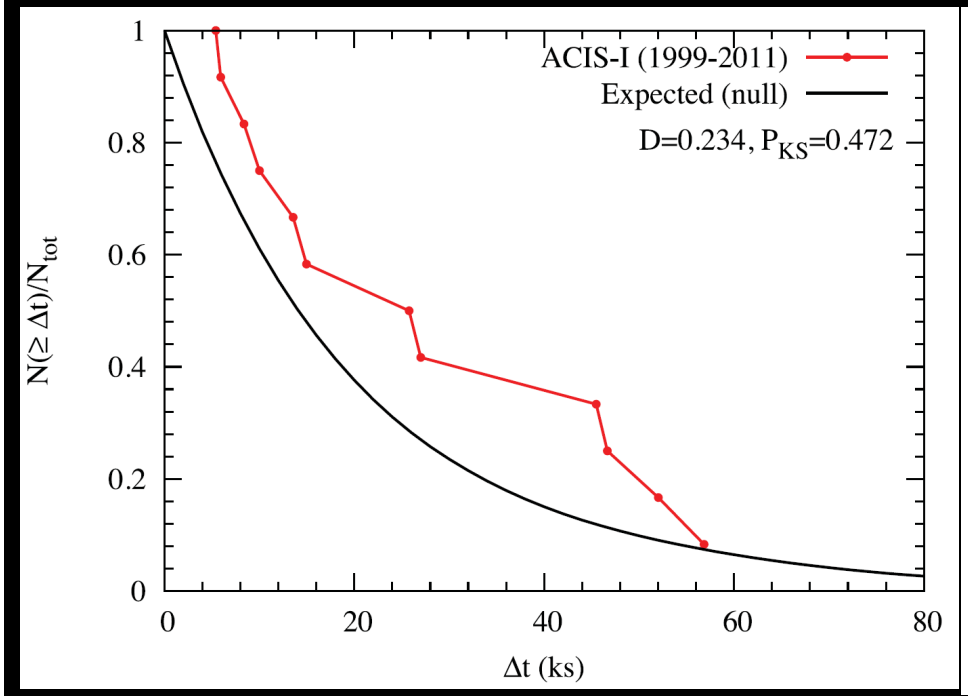

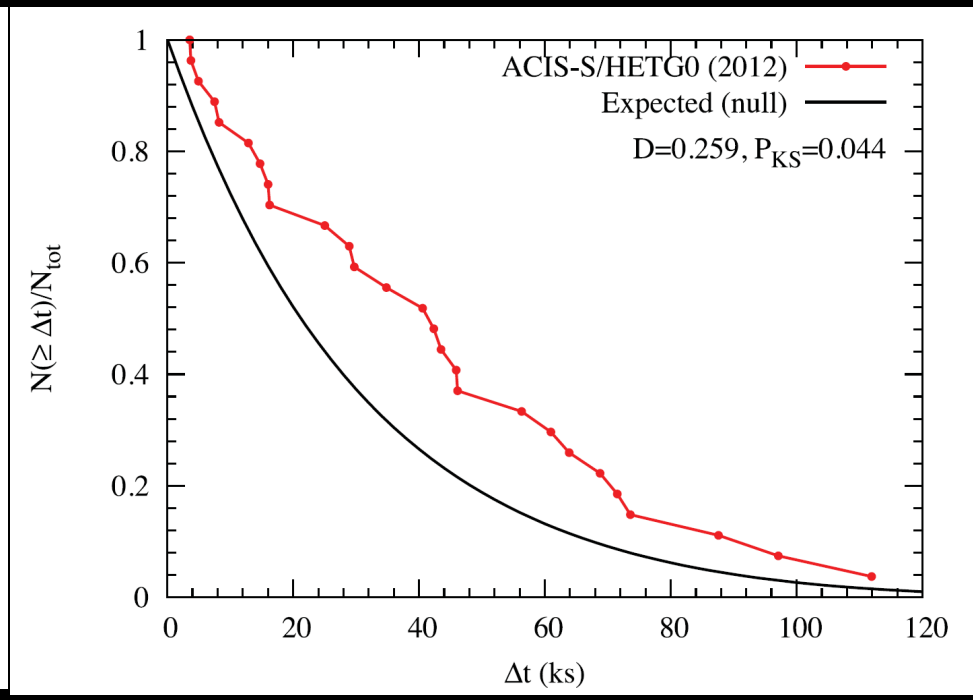

Statistical modeling of the X-ray light curve

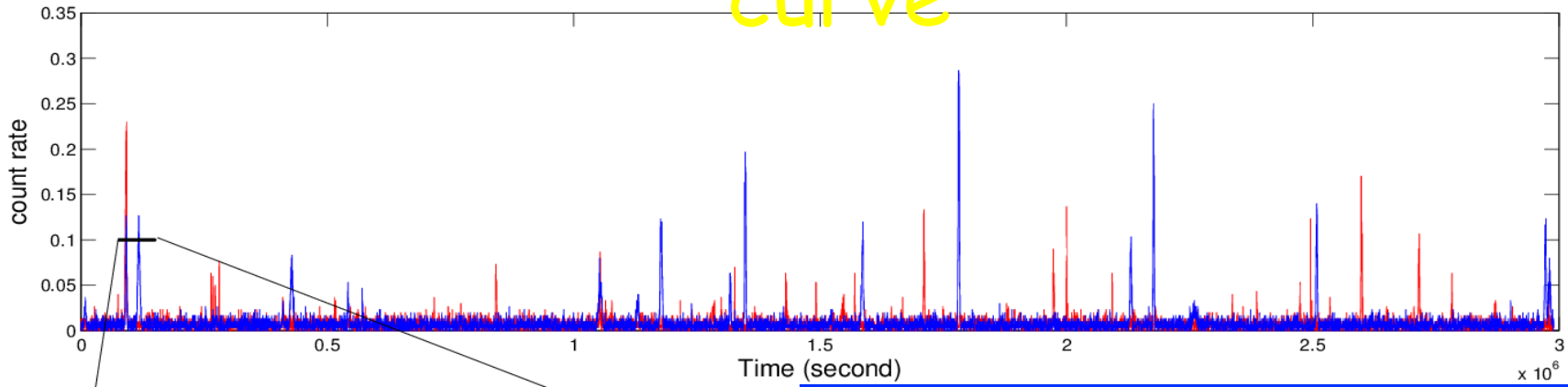

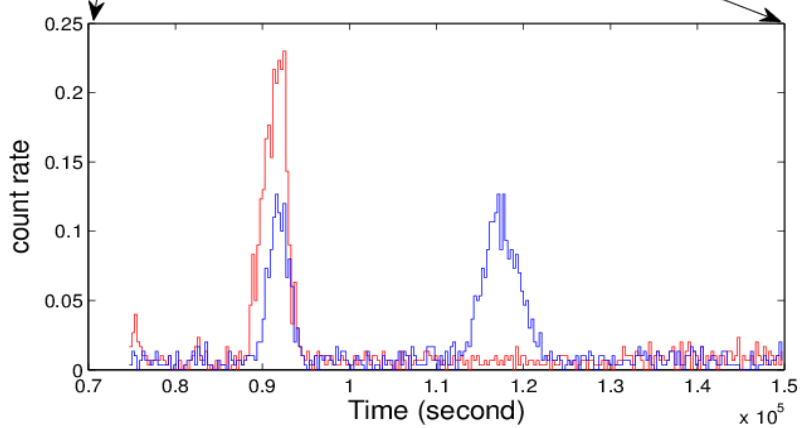

Model light curve into two components:

1. flares with a power law distribution for fluence, *E*:

$$dN/dE \propto \begin{cases} E^{-\alpha_E}, & E_{\min} \le E \le E_{\max} \\ 0, & \text{otherwise} \end{cases}$$

the fluences of the model flares κ

Gaussian flare shape with an energy dependent width:

$$R(t) = \sum_{i=1}^{\kappa} \frac{E_i}{\sqrt{2\pi}\sigma_i} \exp\left[-\frac{1}{2}\left(\frac{t-\mu_i}{\sigma_i}\right)^2\right]$$

$N(\log \sigma_i, \sigma_{ET})$, where $\log \sigma_i = \log A + \alpha_{ET} \log(E_i/100)$

2. a constant quiescent flux r.

Include poisson noise

r, α_E, κ, A, and α_{ET}.

red: observation

blue: simulation

Li, Yuan, Yuan, QDW 2015

MCMC fitting

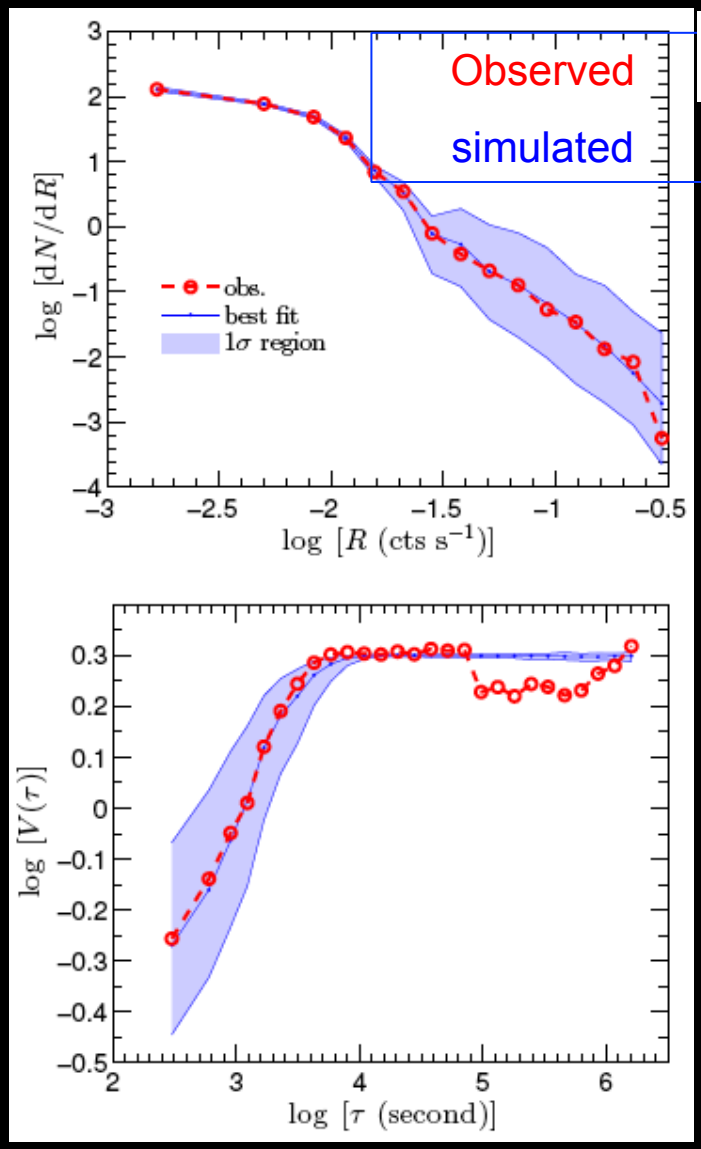

$$\chi^2_{\rm CR} = (\mathbf{n}_{\rm obs} - \mathbf{n}_{\rm sim})^T \mathbf{C}^{-1} (\mathbf{n}_{\rm obs} - \mathbf{n}_{\rm sim}),$$

n_{obs} and n_{sim} are the histograms of the observed and simulated light curves.

Structure function of the light curve:

$$V(\tau) = \frac{\left\langle [R(t+\tau) - R(t)]^2 \right\rangle}{S^2}$$

where R is the X-ray count rate and

$$S^2 = \left\langle \left[R(t) - \overline{R(t)} \right]^2 \right\rangle .$$

Fitting to both the CR distribution and the structure function, accounting for the covariance matrix, by minimizing

$$\chi^2 = \chi^2_{\rm CR} + \chi^2_{\rm SF}$$

$$\chi^2_{\rm SF} = (\log \mathbf{V}_{\rm obs} - \log \mathbf{V}_{\rm sim})^T \mathbf{C}^{-1}_{\rm SF} (\log \mathbf{V}_{\rm obs} - \log \mathbf{V}_{\rm sim})$$

MCMC fitting to the structure function
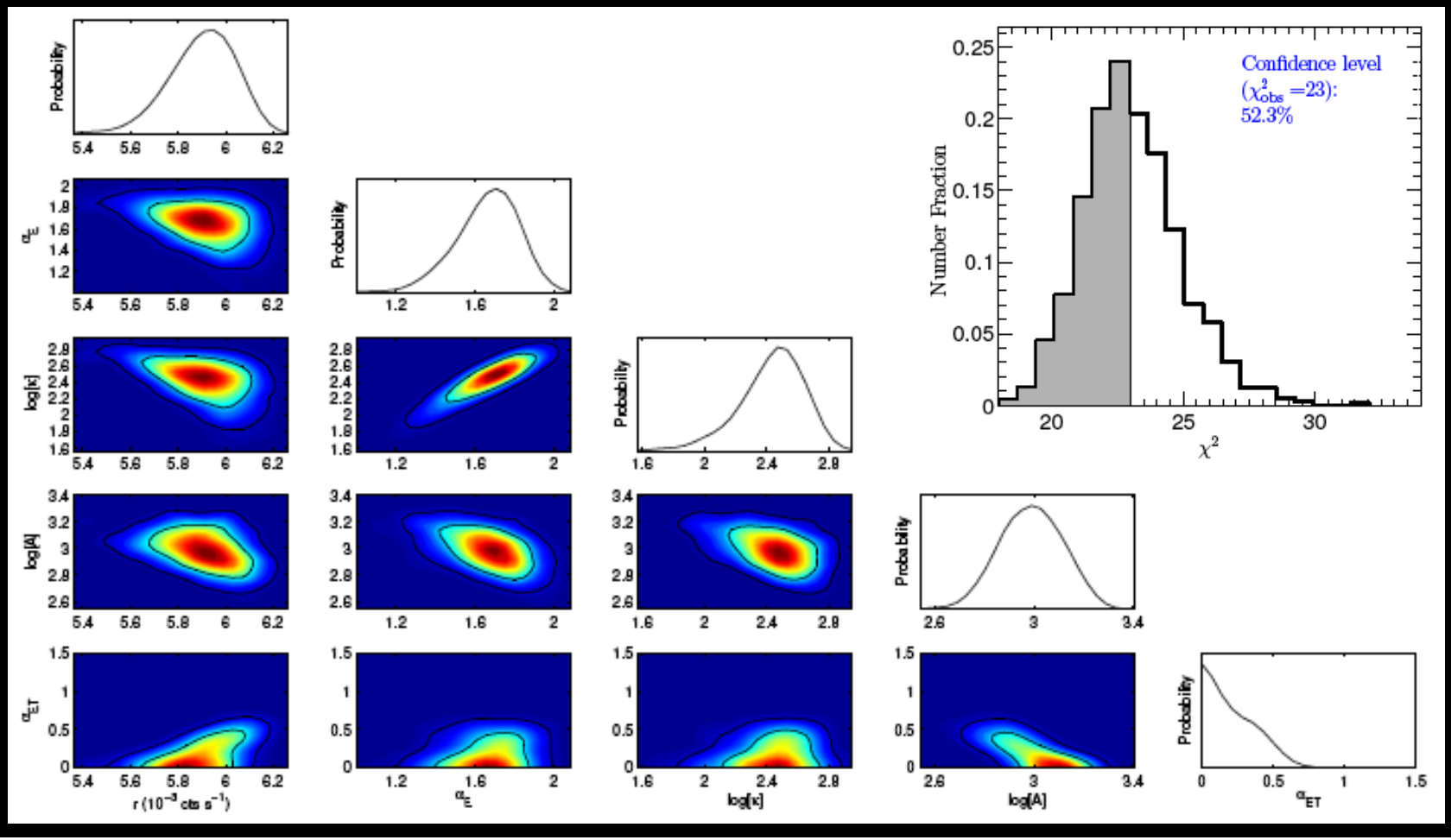
r (10^{-3} cts s^{-1})	α_E	$\log(\kappa)$	$\log(A)$	α_{ET}	χ^2_ν
5.90 ± 0.14	1.66 ± 0.16	2.43 ± 0.21	2.99 ± 0.12	$< 0.52^a$	0.9